Russian Chemical Reviews **71** (5) 383 – 399 (2002) © 2002 Russian Academy of Sciences and Turpion Ltd

DOI 10.1070/RC2002v071n05ABEH000718

High-temperature superconductors based on complex layered copper oxyfluorides †

A M Abakumov, M G Rozova, E I Ardashnikova, E V Antipov

Contents

I.	Introduction	383
II.	Chemical aspects of the synthesis of complex copper oxyfluorides	384
III.	Structural transformations upon fluorination of complex cuprates	386
IV.	Structures, synthesis and superconducting properties of different classes of copper oxyfluorides	387
V.	Conclusion	398

Abstract. Chemical aspects of the synthesis of complex layered copper oxyfluorides possessing superconducting properties or serving as structural matrices for the preparation of new superconductors are discussed. Primary attention is given to fluorination of layered cuprates. Different ways of inserting fluorine into complex copper oxides and the corresponding synthetic approaches are surveyed. The influence of the synthesis conditions on the fluorination pathway, which involves either the incorporation of fluorine or partial replacement of oxygen with fluorine, is analysed. The advantages of xenon difluoride over other fluorinating agents are considered. Fluorination of complex copper oxides often leads to structural changes as exemplified by fluorine-containing phases obtained with the use of both XeF_2 and other fluorinating agents. The bibliography includes 104 references.

I. Introduction

Superconducting materials possess unique properties. The high practical potential of a new generation of high-temperature superconductors, *viz*., complex copper oxides, gave impetus to comprehensive studies of their physical and chemical properties, structural characteristics and 'chemical composition – properties – structure – synthesis conditions' relationships.

The data on the relationships between the composition, structure and properties of numerous copper-containing high-temperature superconducting (HTSC) oxides made it possible to state the following structural and chemical criteria for the appearance of superconductivity:[1]

– the existence of a layered structure composed of weakly distorted or planar superconducting CuO_2 layers, which occur as an infinite network of vertex-sharing CuO_4 squares;

– the presence of optimum interatomic Cu – O distances (ranging from 1.90 to 1.97 Å) in the plane of the conducting layer, which ensure overlapping of the $3d_{x^2-y^2}$-orbitals of copper and the $2p_{x,y}$-orbitals of oxygen to form delocalised states in the σ* band;

– the optimum concentration of charge carriers in the conducting CuO_2 layers must correspond to the ranges of the formal oxidation state of copper from +2.05 to +2.25 and from +1.8 to +1.9 for *p*- and *n*-type superconductors, respectively.

In the structures satisfying these criteria, the negative charge of the CuO_2 layers (if these layers are considered as composed of the Cu^{2+} cations and O^{2-} anions) is compensated by the positive charge of the adjacent nonconducting cationic-anionic charge-reservoir blocks, which offer a means of changing the oxidation state of copper in the CuO_2 layers. By varying the positive charge of these blocks, for example, through either the heterovalent cation substitution or a change in the oxygen content, the required concentration of charge carriers in the conduction band can be achieved. Another way of changing the concentration of charge carriers is to replace a portion of oxygen in the anion sublattice of complex cuprate by fluorine or to insert the fluorine atoms into the structure.

The oxygen and fluorine anions have similar ionic radii (r_{F^-} = 1.29 Å and $r_{O^{2-}}$ = 1.35 Å; for the coordination number of 2; see Ref. 2). Many oxides have structures analogous to those of fluorides and oxyfluorides (for example, CaO and NaF, LaOF and CaF_2, La_2CuO_4 and K_2CuF_4, *etc*.). Consequently, the incorporation of fluorine into complex layered copper oxides can give rise to oxyfluorides structurally similar to these oxides. Fluorine atoms can occupy the anion vacancies or replace oxygen atoms. In both cases, the formal oxidation state of copper is changed. If this incorporation does not lead to destruction or deformation of the CuO_2 layers, the resulting complex oxyfluoride would be expected to exhibit superconducting properties. The superconducting transition critical temperatures (T_c) of some complex copper oxyfluorides are even higher than those of their oxygen analogues (Table 1). Hence, complex layered copper oxyfluorides can be considered as a promising class of compounds for constructing high-temperature superconductors.

Fluorination of complex cuprates not only enables one to achieve the optimum concentration of charge carriers but also offers additional possibilities of searching for new layered compounds. The requirements for the retention of the charge balance and compatibility of interatomic distances in structural fragments (commensurability) impose limitations on the choice of cations involved in nonconducting blocks, which compensate the negative charge of the CuO_2 layers. The replacement of O^{2-} with F^-,

A M Abakumov, M G Rozova, E I Ardashnikova, E V Antipov Department of Chemistry, M V Lomonosov Moscow State University, Leninskie Gory, 119992 Moscow, Russian Federation. Fax (7-095) 939 47 88. Tel. (7-095) 939 52 44. E-mail: abakumov@icr.chem.msu.ru (A M Abakumov), rosova@icr.chem.msu.ru (M G Rozova) Tel. (7-095) 939 55 02. E-mail: ard@inorg.chem.msu.ru (E I Ardashnikova) Tel. (7-095) 939 33 75. E-mail: antipov@icr.chem.msu.ru (E V Antipov)

Received 15 March 2002
Uspekhi Khimii **71** (5) 442 – 460 (2002); translated by T N Safonova

† The review is dedicated to the blessed memory of Professor L M Kovba.

Table 1. Superconducting complex copper oxyfluorides.

Oxyfluoride	T_c /K	Oxygen analogue	T_c /K
$YBa_2Cu_3O_6F_2$	94	$YBa_2Cu_3O_{6.95}$	92
$Y_2Ba_4Cu_7O_{14}F_2$	62	$Y_2Ba_4Cu_7O_{14.92}$	80
$HgBa_2CuO_4F_{0.24}$	97	$HgBa_2CuO_{4.12}$	97
$HgBa_2CaCu_2O_6F_\delta$	128	$HgBa_2CaCu_2O_{6.22}$	127
$Hg_{0.8}Ba_2Ca_2Cu_{3.2}O_8F_\delta$	138	$Hg_{0.8}Ba_2Ca_2Cu_{3.2}O_{8+\delta}$	134
$Sr_2CuO_2F_{2+\delta}$	46	Sr_2CuO_3	–
$La_2CuO_4F_\delta$, $\delta \leqslant 0.18$	35–40	$La_2CuO_{4.032}$	38
$Nd_2CuO_{3.7}F_{0.3}$	27	$Nd_{2-x}Ce_xCuO_4$	24
$Sr_2CaCu_2O_{4.6}F_2$	99	–	–
$Sr_2Ca_2Cu_3O_{6.2}F_{3.2}$	111	–	–
$Sr_2Nd_{0.2}Ca_{0.8}Cu_2O_5F$	85	–	–

whose formal charge is half as large as that of O^{2-}, leads to a decrease in the negative charge of the anion sublattice. Consequently, it is possible to extend the range of cations, which can be involved, together with copper, oxygen and fluorine atoms in compounds showing promise as superconducting materials. At the same time, this difference in the formal charges of the fluorine and oxygen anions requires that the number of fluorine anions be twice as large as that of the oxygen anions to achieve the degree of hole doping in oxyfluorides identical to that in oxygen-containing compounds. The incorporation of hyperstoichiometric anions may lead to substantial structural rearrangements in the parent compound and to changes in its superconducting characteristics.

This review surveys the results both of our studies and investigations of other research groups into the synthesis and structures of complex copper oxyfluorides.

II. Chemical aspects of the synthesis of complex copper oxyfluorides

1. General schemes for the incorporation of fluorine into layered cuprates

For superconducting copper oxyfluorides to be prepared, a particular concentration of holes or electrons in the conduction band must be achieved. The type of charge carriers is determined by the structural features of the starting oxide phase. Let us consider the main processes taking place in the course of fluorination and exerting an effect on the formal oxidation state of copper. There are two schemes for fluorination of complex cuprates giving rise to opposite changes in the oxidation state of copper.

According to one scheme, the oxyfluoride phase is formally considered to be a result of fluorine incorporation into the structure of the oxide prototype, the oxygen contents in both compounds being the same, and an increase in the amount of anions occurring only due to the appearance of additional F^- anions:

$$\underset{\text{oxide phase}}{B_mA_2A'_{n-1}Cu_nO_{2n+2+mx}} + \delta[F] \longrightarrow \underset{\text{oxyfluoride}}{B_mA_2A'_{n-1}Cu_nO_{2n+2+mx}F_\delta},$$

where B is a smaller cation, for example, Hg^{2+}, Bi^{3+}, *etc.*; A and A′ are alkaline-earth and rare-earth cations, respectively; $m = 0, 1, 2$; $n = 1, 2, 3$; $0 \leqslant x \leqslant 1$. (We use the general formula of layered cuprates $B_mA_2A'_{n-1}Cu_nO_{2n+2+mx}$, which reflects the layer sequence

$$\ldots-AO-(BO_x)_m-AO-CuO_2-[A'CuO_2]_{n-1}-AO-(BO_x)_m-AO-\ldots.).$$

The incorporation of fluoride anions leads to an increase in the oxidation state of copper cations (if there are no other cations capable of changing the oxidation state), an increase in the hole concentration and, conceivably, the formation of *p*-type superconductors.

According to another scheme, fluorine atoms partially replace oxygen atoms in the anion sublattice of complex cuprate. The number of oxygen atoms in oxyfluoride generated through anion exchange is smaller than that present in the starting oxide phase, but the overall number of anions remains constant due to the replacement of oxygen atoms with an equivalent amount of fluorine atoms:

$$B_mA_2A'_{n-1}Cu_nO_{2n+2+mx} + \delta[F] \longrightarrow B_mA_2A'_{n-1}Cu_nO_{2n+2+mx-\delta}F_\delta + \delta[O].$$

Heterovalent substitution in the anion sublattice occurs as a reductive process and facilitates the formation of *n*-type superconductors.

The process occurs by predominantly fluorine incorporation or anion exchange, which depend on many factors, for example, on the structure of the initial oxide phase, the procedure for fluorination, temperature and duration of the synthesis. In practice, attempts to carry out fluorination exclusively through one of two paths are not necessarily successful and in most cases the fluorine incorporation and anion exchange proceed simultaneously:

$$B_mA_2A'_{n-1}Cu_nO_{2n+2+mx} + (\delta + \delta')[F] \longrightarrow B_mA_2A'_{n-1}Cu_nO_{2n+2+mx-\delta}F_{\delta+\delta'} + \delta[O].$$

As a result, the oxidation state of copper may remain unchanged but fluorination could lead to the appearance of additional anions in the structure.

2. Methods for the synthesis of layered copper oxyfluorides

The first experiments on the preparation of superconducting oxyfluorides have been carried out by solid-phase reactions. Thus, fluorine was introduced into the starting mixture of carbonates and oxides by the partial replacement of one of the reagents with copper fluoride, alkaline-earth fluoride, rare-earth fluoride, or rare-earth oxyfluoride. The *n*-type superconductor $Nd_2CuO_{4-x}F_x$ was prepared by solid-phase synthesis at 1133–1423 K [NdF_3,[3–7] NdOF (see Ref. 8) or $CuF_2 \cdot 2H_2O$ (see Ref. 9) were used as the source of fluorine]. It should be noted that oxyfluorides $Sr_2MCu_2O_5F_{1+\delta}$ (M = Y, La, Nd, Sm, Gd, Dy, Er or Yb),[10] $Sr_2CaCu_2O_{4+\delta}F_{2\pm y}$ and $Sr_2Ca_2Cu_3O_{6+\delta}F_{2\pm y}$ (see Ref. 11) possessing *p*-type superconductivity were prepared by solid-phase reactions under high pressure (5.5–6 GPa, 1523–1573 K, SrF_2 or CaF_2 as a source of fluorine). Under normal pressure, the high-temperature solid-phase synthesis does not afford fluorine derivatives of complex cuprates if the starting compound contains alkaline-earth cations. In the study,[12] it was reported that the superconducting transition critical temperature for the $YBa_2Cu_3O_yF_x$ compound, which was obtained by the solid-phase reaction involving BaF_2, was increased to 155 K [as compared to $T_c = 90$ K for the oxygen analogue $YBa_2Cu_3O_{6.92}$ (Y123)], but these results were not reproduced in subsequent studies. Moreover, closer examination of the products obtained in the solid-phase synthesis of the fluorine-containing Y123 phase demonstrated that barium fluoride was always present in the final mixture prepared by high-temperature (1073–1223 K) annealing regardless of the form in which fluorine was present in the starting reagents.[13–16]

The high-temperature solid-phase synthesis is also unsuitable for the preparation of other HTSC phases, for example, of $Sr_2CuO_2F_2$. At $\geqslant$753 K, the latter oxyfluoride decomposed to give SrF_2, Sr_2CuO_3 and $Sr_{14}Cu_{24}O_{41}$.[17,18] However, the $Sr_2CuO_2F_{2+\delta}$ compound can be synthesised under much milder conditions (compared to those required for the solid-phase reaction) by treating Sr_2CuO_3 with a gaseous mixture of F_2 (10%) and N_2 (90%) at 483 K for 15 min,[19] with NH_4F in the presence of oxygen at 498 K for 6–8 h,[18,20,21] or with XeF_2 at 433–623 K (from 40 min to 10 h).[17]

Low-temperature fluorination afforded fluorine derivatives of layered cuprates, *viz.*, $YBa_2Cu_3O_{6+\delta}$,[22,23] La_2CuO_4,[24] $M_{2-x}A_{1+x}Cu_2O_{6-\delta}$ (M = La or Nd; A = Ca or Sr),[25] $Pb_2Sr_2YCu_3O_8$,[26] *etc*. Fluorine derivatives of complex cuprates decompose upon heating to form thermodynamically stable products. Their stability is determined primarily by high crystal lattice energies of fluorite-like alkaline-earth fluorides and rare-earth oxyfluorides.

3. Fluorinating agents for the synthesis of fluorine-containing high-temperature superconductors

Low-temperature syntheses of complex copper oxyfluorides were carried out with the use of various fluorinating agents, *viz.*, gaseous fluorine (pure[22,27] or in mixtures with other gases[19,24]), NF_3,[23] NH_4F,[28–31] NH_4HF_2,[32,33] transition-metal fluorides (ZnF_2, CuF_2, NiF_2, AgF_2)[34–38] and ClF_3.[39,40]

Xenon difluoride, which offers promise as a fluorinating agent, was first proposed for fluorination of HTSC cuprates in the study.[17] This reagent has advantages over other reagents. At room temperature, XeF_2 is a solid compound, which enables one to use it in precise amounts and, hence, to attain the required degree of fluorination and the desired oxidation state of copper. Xenon difluoride is much less aggressive than gaseous fluorine due to which no expensive bulky apparatus is required. In addition, xenon difluoride does not generate by-products that contaminate the sample synthesised.

Xenon difluoride serves as an oxidising agent, unlike ammonium fluoride, which creates reductive conditions and leads to an increase in the oxidation state of copper only in the reactions performed in the presence oxygen[18,30] or through disproportionation of the reaction products to form oxidised and reduced phases.[20]

Many transition-metal fluorides $M'F_2$ (M′ = Hg or Ag), like XeF_2, are oxidising fluorinating agents. However, the reactions with the use of these compounds not only lead to fluorine incorporation but can also be accompanied by anion substitution, the probability of the latter being increased as the reaction temperature is raised. Fluorination with $M'F_2$ (M′ = Zn, Cu or Ni) proceeds predominantly according to the reaction

$$\delta M'F_2 + B_mA'_2A''_{n-1}Cu_nO_{2n+2+mx} \longrightarrow \longrightarrow \delta M'O + B_mA'_2A''_{n-1}Cu_nO_{2n+2+mx-\delta}F_{2\delta},$$

In this case, the oxidation state of copper remains unchanged. When the exchange reactions are performed by direct mixing of $M'F_2$ with the compound to be fluorinated rather than being carried out in the gas phase, impurities of metal oxide contaminate the resulting sample.

4. Use of XeF_2 as a fluorinating agent in the synthesis of fluorine-containing high-temperature superconductors

Trace amounts of water, which are, for example, adsorbed on the powdered starting compounds, contaminate fluorination products due to pyrohydrolysis. Hydrogen fluoride, which is evolved in the reactions of XeF_2 or oxyfluoride that formed with water, reacts with the starting oxide or oxyfluoride with elimination of water. The latter is again involved in pyrohydrolysis.[17] For example,

$$Sr_2CuO_3\ [\text{or } Sr_2Cu(O,F)_{4+\delta}] + HF \longrightarrow SrF_2 + CuO + H_2O,$$

$$Sr_2Cu(O,F)_{4+\delta} + H_2O \longrightarrow SrF_2 + Sr_2CuO_3 + CuO + HF.$$

Fluorination at high temperatures must be carried out in hermetically sealed containers resistant to fluorine because it is necessary, first, to exclude exposure to water vapour and, second, to prevent leakage of xenon difluoride that has high volatility. We developed an original procedure for fluorination. According to this procedure, the reactions are carried out in a sealed nitrogen-filled copper tube in which a nickel crucible containing a mixture of the starting compound and XeF_2 is placed. (All operations associated with the preparation of samples must be performed in a dry chamber.) In the temperature range of 423–673 K, XeF_2 exists predominantly in the gas phase and reacts with complex oxides through a gas–solid mechanism. Calculations of the temperature dependence of the equilibrium composition of the gas mixture (using the database[41]) containing one mole of XeF_2 at 1 atm (Fig. 1) demonstrated that at temperatures below 673 K this mixture is composed of Xe, XeF_2 and XeF_4 as the major components, the last two compounds serving as fluorinating agents. Xenon tetrafluoride surpasses xenon difluoride in oxidising activity[42,43] but its concentration in the gas mixture at $T < 673$ K is much lower than the concentration of XeF_2. At reaction temperature higher than 673 K, dissociation of XeF_2 into F_2 and Xe becomes noticeable.

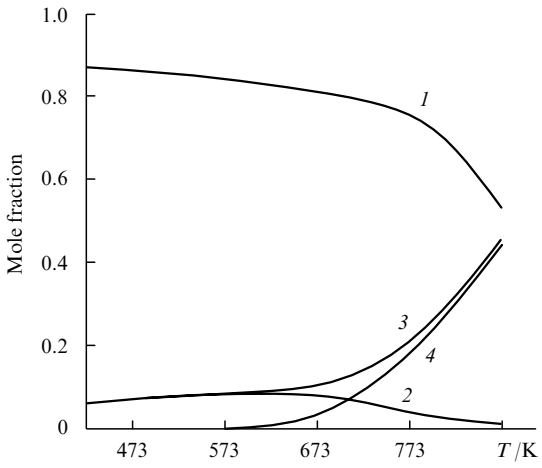


Figure 1. Temperature dependence of the equilibrium composition of the gas mixture containing one mole of XeF_2 at 1 atm.[41] (*1*) XeF_2, (*2*) XeF_4, (*3*) Xe, (*4*) F_2.

Fluorination with xenon difluoride in different temperature ranges involves the following main reactions. It was demonstrated[44] that the incorporation of fluorine into the structure of complex cuprate was the major process in the case of fluorination of $YBa_2Cu_3O_{6.11}$ (Y123 phase) in the temperature range from 423 to 573 K

$$YBa_2Cu_3O_{6.11} + 0.5x\,XeF_2 \longrightarrow YBa_2Cu_3O_{6.11}F_x + 0.5x\,Xe.$$

This reaction led to an increase in the formal oxidation state of copper from +1.74 in the starting strongly reduced phase $YBa_2Cu_3O_{6.11}$ to +2.03–+2.14 in the fluorinated samples. When the temperature was increased to 673 K, competitive anion exchange took place, *i.e.*, oxygen atoms were partially replaced by fluorine atoms. The anion exchange causes partial reduction of copper cations because the formation of the fluorinated phase is accompanied by the replacement of one O^{2-} anion with one F^- anion. It is impossible to distinguish unambiguously the temperature ranges in which the fluorine incorporation and anion exchange proceed autonomously. Both competitive processes occur simultaneously

$$YBa_2Cu_3O_{6.11} + 0.5(y+x)\,XeF_2 \longrightarrow \longrightarrow YBa_2Cu_3O_{6.11-y}F_xF_y + 0.5(y+x)\,Xe + y\,[O].$$

It can only be noted that the anion exchange is enhanced as the temperature is increased and finally dominates over fluorine incorporation. Thus, the reaction of the oxidised phase $YBa_2Cu_3O_{6.95}$ with XeF_2 at 623 K led to a decrease in the oxidation state of copper from +2.30 to +2.22, which is indicative of the formation of a more reduced phase, *i.e.*, of the partial replacement of oxygen with fluorine. Oxygen evolved in the course of this process is absorbed by the walls of a copper tube to form Cu_2O due to which it cannot act as an oxidiser. At 603 K,

the partial pressure of oxygen in the tube [$\ln P_{O_2} = -22.2$ (atm)], which corresponds to the equilibrium pressure of oxygen over a mixture of Cu and Cu_2O at this temperature, is comparable to the partial pressure of oxygen over the strongly reduced phase $YBa_2Cu_3O_{6.1}$ [$\ln P_{O_2} = -21.1$ (atm)] at the same temperature.[44]

Nevertheless, the process can be forced to occur predominantly either by fluorine incorporation or anion exchange by changing the temperature range. This can be used for choosing the method of doping to create *p*- or *n*-type superconductors. The final step of the anion exchange involves the destruction of the structure of complex copper oxide (in the temperature range of 673–773 K) under the action of xenon difluoride or fluorine generated upon decomposition of the former:

$$YBa_2Cu_3O_6 + 2.5\,XeF_2 \longrightarrow YOF + 2BaF_2 + 3CuO + 2.5\,Xe + 2[O],$$

$$YBa_2Cu_3O_6 + 2.5\,F_2 \longrightarrow YOF + 2\,BaF_2 + 3\,CuO + 2\,[O].$$

III. Structural transformations upon fluorination of complex cuprates

As mentioned above, oxygen and fluorine have similar ionic radii and the simple replacement of oxygen atoms by an equivalent amount of fluorine atoms would not lead to substantial structural changes of complex oxyfluoride copper compared to that of complex oxide but must be accompanied by a decrease in the formal oxidation state of copper. As an example, we refer to the $Nd_2CuO_{4-x}F_x$ solid solutions, which have tetragonal structures of the T' phase (Nd_2CuO_4) (Fig. 2). An increase in the degree of replacement of O atoms by F atoms is accompanied by an increase in the unit cell parameter *a* because a reduction in the formal oxidation state of copper leads to an increase in the occupancy of the antibonding σ* band and elongation of the equatorial $Cu-O_{eq}$ bond. Simultaneously, the structure is slightly contracted along the *c* axis, which is probably associated with the difference in the ionic radii of oxygen and fluorine.[4, 28]

Studies of fluorinated samples by near-edge X-ray absorption fine structure (NEXAFS) spectroscopy demonstrated that fluorine atoms replace oxygen atoms in the tetrahedrally coordinated positions of the fluorite-like Nd_2O_2 block.[45] Distortions of the crystal structures of the $Nd_2CuO_{4-x}F_x$ and $Nd_{2-x}Ce_xCuO_4$ solid solutions were examined by the electron diffraction method and high-resolution transmission electron microscopy (HRTEM).[46] The observed various superstructures of fluorine-containing compounds were identical with those of cerium-substituted compounds. These superstructures resulted, apparently, from ordering of the anions and anion vacancies, which were generated upon annealing of the samples at 523–1023 K *in vacuo*, rather than were associated with the replacement of oxygen by fluorine. The examination of the superconducting $Nd_2CuO_{3.8}F_{0.2}$ sample by the HRTEM method did not reveal a superstructure for this compound.[4]

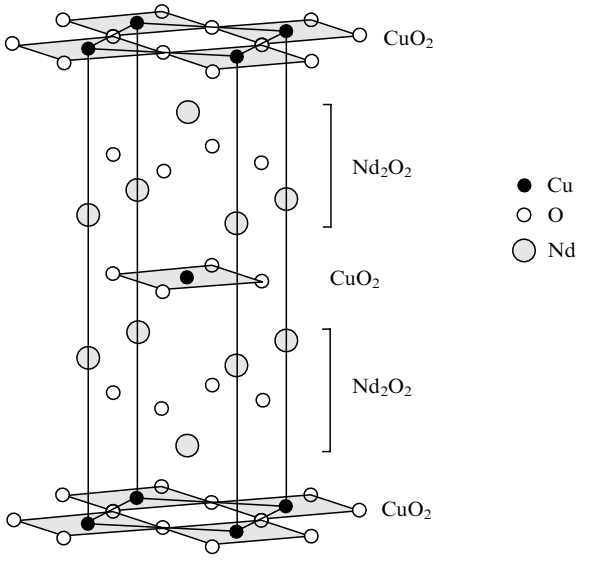


Figure 2. Crystal structure of Nd_2CuO_4.

The appearance of hyperstoichiometric anions in the structure due to fluorine incorporation or the replacement of O^{2-} anions with a double amount of F^- ions can lead to structural transformations involving changes in the coordination polyhedra, interatomic distances and space symmetry up to the complete rearrangement of the crystal structure. For example, strontium cuprate Sr_2CuO_3 is structurally similar to La_2CuO_4. However, unlike the crystal structure of the latter, which consists of the CuO_2 layers, the crystal structure of Sr_2CuO_3 is composed of chains of the vertex-sharing CuO_4 squares (Fig. 3 *a*) due to ordering of the oxygen atoms and anion vacancies. Hence, the composition of the layer can be written as CuO□. Fluorination of Sr_2CuO_3 caused the rearrangement of the oxygen atoms and their migration from the Sr_2O_2 block to the equatorial coordination environment about the copper atoms.[19, 47] As a consequence, complex oxyfluoride $Sr_2CuO_2F_{2+\delta}$ contains the conducting CuO_2 layers (Fig. 3 *b*). As a result of incorporation of additional fluorine atoms into the tetrahedral cavities of the Sr_2O_2 block, the concentration of holes in the conduction band became higher than the optimum value. However, the required doping level was achieved upon subsequent reductive annealing and the compound was transformed into the superconducting state at 46 K. The partial replacement of strontium with barium to form the $Sr_{2-x}Ba_xCuO_2F_{2+\delta}$ solid solution made it possible to increase T_c to 64 K ($x = 0.6$).[20] Calculations of the energy of Coulombic interactions [19, 47] suggested that the driving force for the anionic rearrangement is the difference between the lattice energy of the compound which contains fluorine atoms in the axial vertices of the octahedra about the copper atoms and the lattice energy of the same compound which contains the fluorine atoms in the equatorial positions to form the CuOF layers.

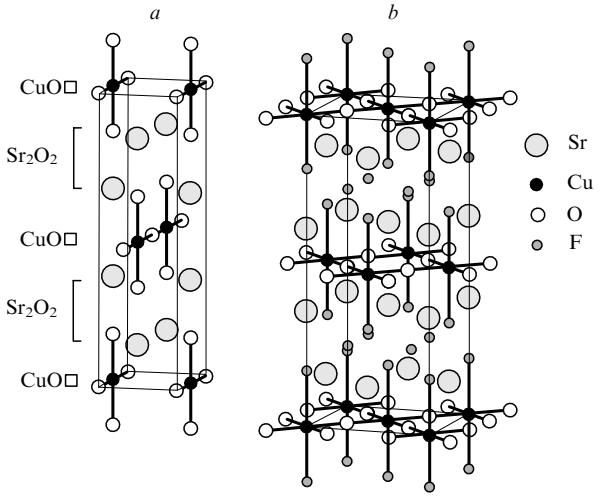


Figure 3. Crystal structures of Sr_2CuO_3 (*a*) and $Sr_2CuO_2F_{2+\delta}$ (*b*).

The incorporation of additional anions into vacancies of the anion sublattice of the $B_mA_2A'_{n-1}Cu_nO_{2n+2+mx}$ compounds leads to an increase in the coordination number of the B cations, which was initially smaller than 6. If these cations are Cu^{2+}, the completion of their coordination environment to an octahedron must lead to deformation of the crystal structure accompanied by an increase in the distance between the layer containing the copper cations and the adjacent layers containing the A cations. The $Cu(O,F)_6$ octahedron is tetrahedrally distorted due to the

Jahn–Teller effect resulting from the unsymmetrical occupancy of the e_g level ($3d^2_{z^2}3d_{x^2-y^2}1$). As a consequence, the $Cu-O_{ax}$ distance becomes substantially larger than the $Cu-O_{eq}$ distance resulting in an increase in the interlayer distances in the structure. Thus, the formation of an octahedron about the copper atoms in $Sr_2CuO_2F_{2+\delta}$ leads to a substantial increase in the unit cell parameter c (c = 13.468 Å)[19] as compared to that observed in the initial compound Sr_2CuO_3 (a = 12.716 Å).[48]

If the B sublattice contains cations whose stable coordination number is smaller than 6, for example, the Ga^{3+} cations in the tetrahedral environment in the Ga1201 ($MACuGaO_5$, M = La, Pr or Nd; A = Ca or Sr)[49,50] and Ga1212 ($Y_{0.6}Ca_{0.4}Sr_2Cu_2GaO_7$) phases,[51] the crystal structures, including the CuO_2 layers, may be distorted due to ordering of the oxygen atoms and anion vacancies in the $B(O,\square)_2$ layers. Deformation of the structure may be responsible for the absence of superconducting properties. The filling of vacancies with additional anions upon fluorination leads to a reduction in deformations up to the formation of a structure characterised by a higher space symmetry group and undeformed conducting layers. The same effect would be expected to occur when fluorination causes changes in the sizes of the structural blocks in the plane of the CuO_2 layers, which are favourable for the establishment of their commensurability and removal of structural distortions appearing upon adaptation of the structural blocks to each other. The incorporation of fluorine atoms into the interlayer cavities of the structure with the completed anion sublattice would, most probably, lead to lowering of the symmetry due to displacement of the atoms from the ideal positions, thus minimising Coulombic repulsions between the anions in the interlayer cavities and the anions in the adjacent atomic layers.

Hence, the superconducting properties of complex copper oxyfluorides are determined not only by the character of changes in the oxidation state of copper through different mechanisms of fluorination but also by possible structural transformations.

IV. Structures, synthesis and superconducting properties of different classes of copper oxyfluorides

1. Fluorination of the $MBa_2Cu_3O_{6+\delta}$ (M = Y, Dy, Ho, Tm) and $Y_2Ba_4Cu_7O_{14+\delta}$ phases

The perovskite-like anion-deficient structures of the $MBa_2Cu_3O_{6+\delta}$ phases (M123 phase) with unit cell parameters $a \approx b \approx a_p$, $c \approx 3a_p$, where a_p is the parameters of the perovskite sublattice (Fig. 4 *a*), involve the following layer sequence

$$-Cu\square O_\delta - BaO - CuO_2 - M\square - CuO_2 - BaO - Cu\square O_\delta -$$

($\square$ is the anion vacancy).

The anion positions in the $Cu\square O_\delta$ layer (Cu1 layer) can be completely vacant at $\delta = 0$, which corresponds to the structure of the tetragonal strongly reduced M123 phase. The latter does not possess superconducting properties (the formal oxidation state of copper is +1.67). The Cu1 atoms (see Fig. 4 *a*) have a dumbbell-like coordination typical of the Cu^+ cations. At $\delta \approx 1$, the oxygen atoms occupy half of the vacancies in the Cu1 layer in an ordered fashion thus completing the coordination environment about the copper atoms to a square. The chains of the vertex-sharing CuO_4 squares are oriented along the *b* axis resulting in an orthorhombic distortion of the structure. The hole concentration in the compounds with $\delta \approx 1$ is close to the optimum value and these compounds have the highest superconducting transition temperatures (T_c = 92–94 K) of all $MBa_2Cu_3O_{6+\delta}$ compounds.

The $Y_2Ba_4Cu_7O_{14+\delta}$ compound (Y247 phase) is structurally related to $YBa_2Cu_3O_{6+\delta}$ (Y123) with the difference that the former structure contains chains consisting of the doubled copper–oxygen squares (see Fig. 4 *b*). In the structures of both phases, the fluorine atoms can occupy the anion positions of the Cu1 layer instead of the oxygen atoms. Fluorination of samples of the Y123 phase characterised by different oxygen contents was examined in numerous studies. The results of these investigations are briefly summarised below.

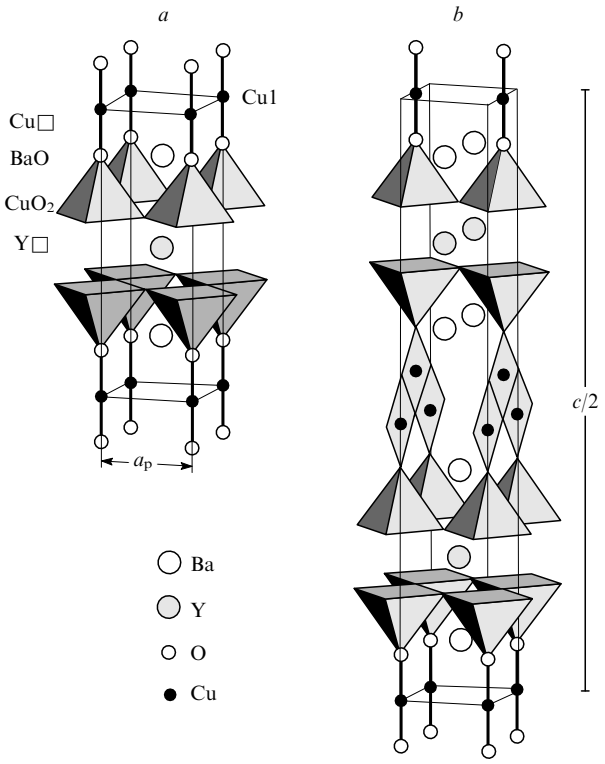


Figure 4. Crystal structures of $YBa_2Cu_3O_6$ (*a*) and $Y_2Ba_4Cu_7O_{14}$ (*b*).

Fluorine is incorporated into the structures of partially reduced or completely oxidised $YBa_2Cu_3O_{6+\delta}$ samples ($\delta \geqslant 0.65$) and occupy vacancies in the Cu1 layer both along the *a* and *b* directions of the orthorhombic unit cell. The positions are occupied successively. In the case of a low degree of fluorination, the fluorine atoms occupy predominantly the position (0, 1/2, 0). Powder neutron-diffraction studies demonstrated[52] that once the occupancy of this position reached 80%, the incorporation of the fluorine atoms into the position (1/2, 0, 0) started. This scheme of filling the positions is consistent with the fact that the orthorhombic distortion of the unit cell was enhanced for $YBa_2Cu_3O_{6.7}F_{0.15}$ and was subsequently reduced for $YBa_2Cu_3O_{6.7}F_{0.3}$. Fluorination of $YBa_2Cu_3O_{6.7}$ led to an increase of T_c from 65 to 90 K.

Fluorination of a strongly reduced $YBa_2Cu_3O_{6.2}$ sample by the electrochemical method caused the orthorhombic distortion of its tetragonal structure.[53] The fluorine incorporation gave rise to a blurred superconducting transition with T_c = 55–60 K, which is similar to T_c for $YBa_2Cu_3O_{6.5}$.

In most cases, fluorination of the strongly oxidised $YBa_2Cu_3O_{6+\delta}$ phase with δ nearly-unity allows one to prepare compounds possessing T_c no higher than that achieved for the optimally oxygen-doped sample.[22,23,53,54] However, it was reported that the treatment of $YBa_2Cu_3O_{6+\delta}$ with a mixture of nitrogen and fluorine led to an increase of T_c from 92 to 96 K.[55]

An increase in the degree of fluorination of the starting phase Y123 gave rise to a fluorinated phase with a tetragonal unit cell regardless of the hyperstoichiometric oxygen content.[53,56] Fluorination, like the oxygen incorporation, was accompanied by the contraction of the structure along the *c* axis. This indicates that the copper atoms in the fluorinated and oxygen-doped Y123 phases have similar coordination environments and that anion vacancies are abundant in the Cu1 layer, which is retained even in the case of a high degree of fluorination. As exemplified by the $YBa_2Cu_3O_{6.65}$ sample treated with NF_3,[56] tetragonal symmetry occurs due to the

fact that the positions (1/2, 0, 0) and (0, 1/2, 0) are statistically occupied by the anions (the occupancies of the positions are 68%).

Kistenmacher predicted [57] the existence of complex oxyfluoride $YBa_2Cu_3O_6F_2$. In the structure of this compound, the anion vacancies in the Cu1 layer are completely filled with fluorine atoms. In this compound, the oxidation state of copper must be equal to +2.33, which is identical to that observed in $YBa_2Cu_3O_7$ (oxygen-doped Y123 phase). Oxyfluoride would be expected to have tetragonal symmetry (due to the replacement of the copper–oxygen chains with the two-dimensional CuF_2 layers) and exhibit superconducting properties. Evidently, the parameter c of the tetragonal unit cell of complex oxyfluoride $YBa_2Cu_3O_6F_2$ must be substantially larger than the analogous parameter of the oxide phase due to manifestation of the Jahn–Teller effect in the CuO_2F_4 octahedra.

For complex oxyfluoride $YBa_2Cu_3O_6F_2$ to be formed, the Cu1 layers in the starting compound must contain as few oxygen atoms as possible. Fluorination of the reduced nonsuperconducting $YBa_2Cu_3O_{6.11}$ compound led to substantial changes in the X-ray diffraction pattern, an increase in the oxidation state of copper to +2.14 and the manifestation of superconductivity at 94 K (the volume of the superconducting phase was ~25%). The X-ray diffraction pattern of the fluorinated compound is characterised by the presence of sharp intense reflections with the Miller indices $hk0$. The general reflections hkl are virtually absent. Relying on these data, only the parameter $a = 3.869$ Å of the tetragonal unit cell of the fluorinated compound was determined, the existence of strong disorder was proposed and the occurrence of numerous defects along the c direction was suggested.[44]

The structure of the fluorinated sample was examined by the HRTEM method in combination with electron probe X-ray analysis, which confirmed the presence of fluorine in crystallites. The electron diffraction pattern and images obtained by the HRTEM method (Fig. 5) are unambiguously indicative of the formation of a new compound with unit cell parameters $a \approx 3.87$ Å and $c \approx 13$ Å.[58]

In the crystallites, the domains of this compound (F2 phase) or extended defects alternate with the domains of the starting structure (F1 phase). Electron probe X-ray analysis demonstrated that the fluorine content in the F2 phase is much higher than that in the F1 phase (the precise fluorine content is impossible to determine by this method). Substantial broadening and a decrease in the intensities of the lines with the non-zero Miller indices l in X-ray diffraction experiments are accounted for by small sizes of the domains along the [001] direction. A comparison of the experimentally observed contrast in the images obtained by the HRTEM method with the results of calculations using different structural models allowed the conclusion that an increase in the parameter c for the F2 phase is associated with an increase in the distance between the BaO and Cu1 layers (but not in the distance between the CuO_2 and $Y\square$ layers). On this basis, it was suggested that the fluorine atoms are incorporated into the anion vacancies

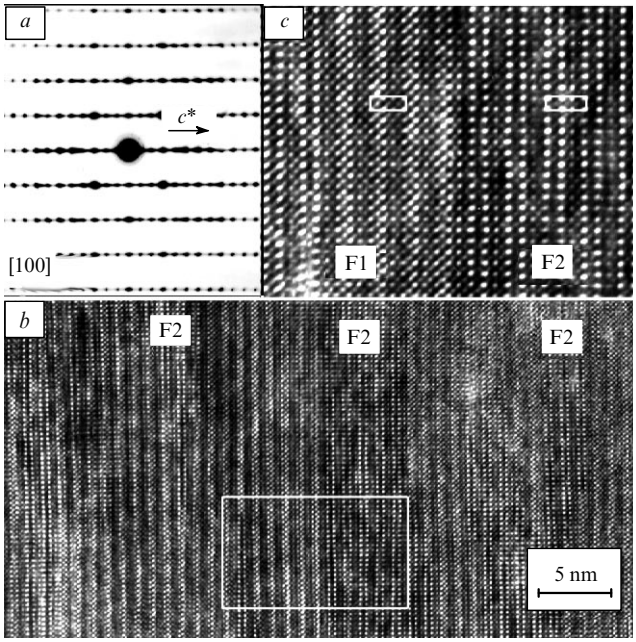


Figure 5. Images along the [100] direction obtained by electron diffraction (*a*) and HRTEM (*b*, *c*) methods. The sample was prepared by the treatment of $YBa_2Cu_3O_{6.11}$ with xenon difluoride at 623 K for 50 h.

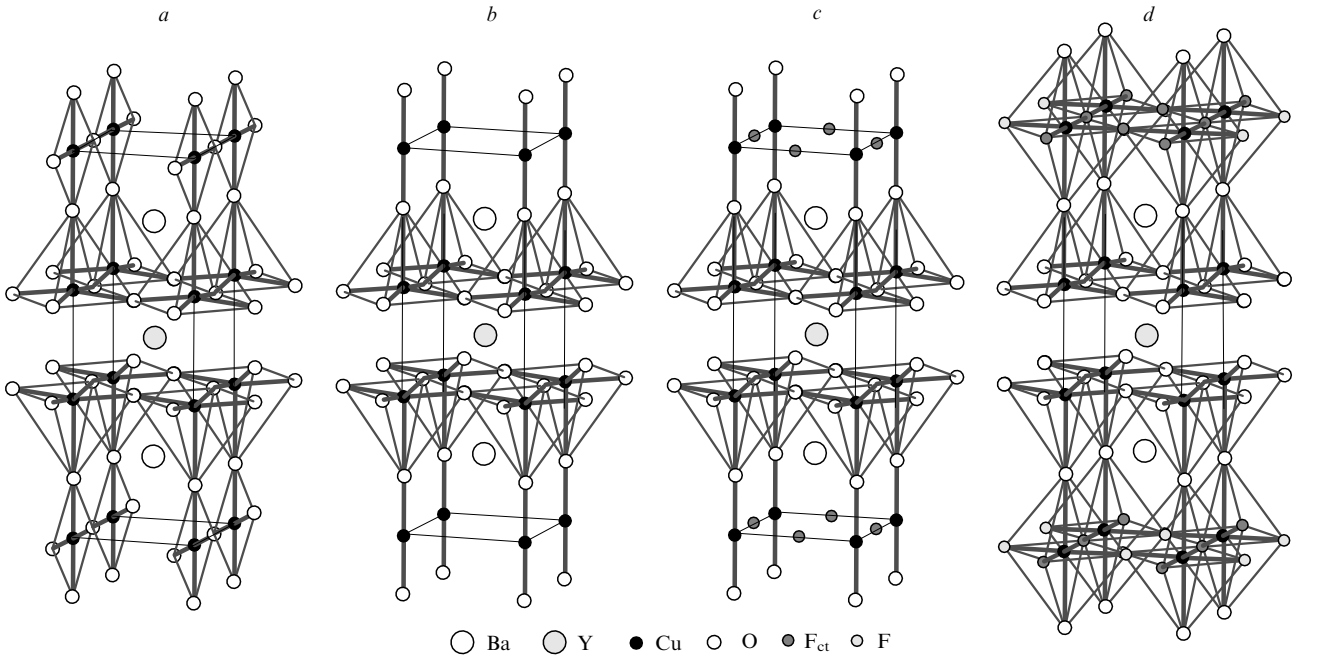


Figure 6. Scheme of the structural transformations in the Y123 phase upon oxygen and fluorine incorporation. (*a*) $YBa_2Cu_3O_7$; (*b*) $YBa_2Cu_3O_6$; (*c*) $YBa_2Cu_3O_6F$; (*d*) $YBa_2Cu_3O_6F_2$.

in the Cu1 layer, which is accompanied by the formation of the distorted CuO_2F_4 octahedra. According to the proposed structural model, elonagtion of the axial Cu–O distance from 1.85 Å in the initial compound $YBa_2Cu_3O_{6.11}$ to 2.3–2.5 Å in the fluorinated sample must lead to the parameter c of 12.8–13.2 Å in the $YBa_2Cu_3O_6F_2$ structure. The results of an electron microscopic study confirmed this suggestion and provided support for the fact that new superconducting oxyfluoride with composition $YBa_2Cu_3O_6F_2$ was synthesised. The scheme of the structural transformations caused by the incorporation of the oxygen and fluorine atoms into the tetragonal $YBa_2Cu_3O_6$ structure is shown in Fig. 6.

Upon fluorination, the properties of the $Y_2Ba_4Cu_7O_{14+\delta}$ (Y247 phase) compound are changed in much the same manner. The incorporation of fluorine atoms into the structure of strongly reduced oxide $Y_2Ba_4Cu_7O_{14.09}$ led to a rise in T_c from 30 to 62 K and an increase in the unit cell parameter c from 50.6 to 53.5 Å.[59] The fluorinated Y247 phase, unlike the fluorinated Y123 phase, remains orthorhombic because fluorination has no effect on the chains formed by the doubled copper–oxygen CuO_4 squares although the degree of orthorhombic distortion is somewhat lowered.

Investigation by the HRTEM method demonstrated that the incorporation of the fluorine atoms into the Y123 and Y247 phases occurred non-homogeneously. The completely fluorinated phase with composition $YBa_2Cu_3O_6F_2$ was found as extended domains in a matrix of the partially fluorinated Y123 phase. In the fluorinated Y247 phase, the regions in which the positions in the Cu1 layer are completely occupied by the fluorine atoms occur only as local defects (Fig. 7). An analogous microstructure was found in the fluorinated $MBa_2Cu_3O_{6.12}$ phases (M = Dy, Ho or Tm).[60] Unlike the Y123 phase, the reactions of the M123 phases with XeF_2 proceed predominantly through a mechanism of anion exchange due to which it is impossible to achieve the oxidation state of copper suitable for the manifestation of superconductivity.

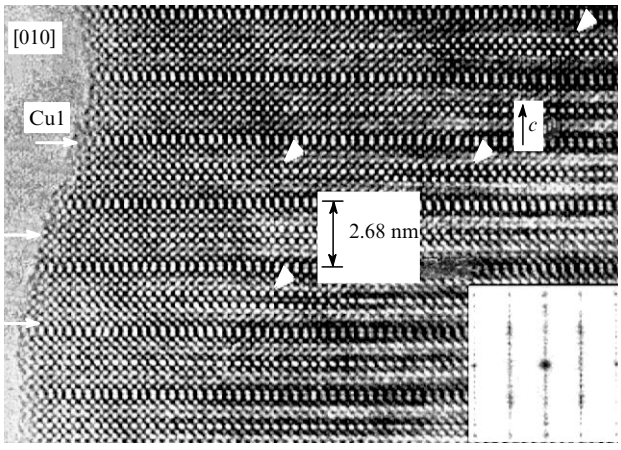


Figure 7. HTREM image of the [010] zone. Local defects, which are inclusions of the $Y_2Ba_4Cu_7O_{14}F_2$ phase, are indicated by arrows. The optical-diffraction image is shown in the lower inset at the right of the illustration.

2. Fluorine derivatives of mercury-containing superconducting cuprates $HgBa_2CuO_{4+\delta}$ (Hg1201) and $Hg_{0.8}Ba_2Ca_2Cu_{3.2}O_{8+\delta}$ (Hg1223)

Fluorine atoms incorporated into the Y123 structures and related phases form strong bonds with the copper cations in the Cu1 layers thus changing their coordination environment and interatomic distances (Fig. 8). The structures of mercury-containing cuprates are characterised by the presence of the anion position (1/2, 1/2, 0) in the mercury-containing layer. This position can be

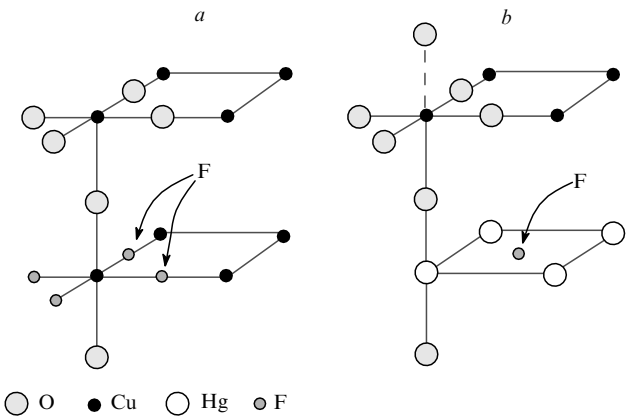


Figure 8. Scheme of incorporation of fluorine atoms into the structures of the phases Y123, Y247 (*a*) and Hg1201, Hg1223 (*b*).

partially occupied by oxygen or fluorine atoms, thus changing the hole concentration in the conduction band. The stable dumbbell-like coordination of the Hg^{2+} cations is responsible for the absence of steric hindrances as well as for weak interactions between these anions and the mercury cations. Due to the formation of the long weak Hg–O(F) bond in the plane of the layer, the incorporation of anions into this layer cannot induce substantial structural changes, which were observed in the Y123 and Y247 phases.[61] A comparative analysis of the properties of samples oxidised with fluorine or oxygen (the anion contents, the formal oxidation states of copper, structural parameters and the superconducting transition temperatures were compared) allowed important conclusions about the nature of superconductivity in mercury-containing cuprates.

Early experiments on the synthesis of the fluorinated Hg1212 and Hg1223 phases were performed with the use of BaF_2 (Ref. 62) or CuF_2 (Ref. 63) as a source of fluorine. The experiments were carried out at high temperatures (923–1073 K). These syntheses afforded multiphase samples, which contained superconducting phases with unit cell parameters similar to those of the corresponding phases in oxygen-saturated samples.

The reactions of mercury-containing cuprates with xenon difluoride proceeded at rather low temperatures (423–473 K), which made it possible to perform fluorination predominantly through fluorine incorporation, the probability of anion exchange being substantially decreased. Fluorination of the strongly reduced $HgBa_2CuO_{4.01}$ phase with T_c = 61 K led to a change in the superconducting transition critical temperature. At low degrees of fluorination, T_c reached maximum value of 97 K and then decreased. In the case of too high oxidation states (overdoping) of copper, the superconductivity can be completely suppressed.[64] The aforesaid is illustrated by the following example:

$$HgBa_2CuO_{4.01} \xrightarrow{0.3\ XeF_2} HgBa_2CuO_4F_{0.24} \xrightarrow{0.4\ XeF_2} HgBa_2CuO_4F_{0.32}$$

a = 3.8915(5) Å,	a = 3.8825(3) Å,	a = 3.8724(4) Å,
c = 9.529(2) Å,	c = 9.510(1) Å,	c = 9.493(2) Å,
T_c = 61 K	T_c = 97 K	T_c = 80 K

The presence of fluorine atoms in the mercury-containing layer was unambiguously established by ^{19}F NMR spectroscopy.[65,66] The possible distribution of the atoms over the crystallographic positions in these structures can be judged from the temperature dependences of the rates of ^{19}F spin–lattice relaxations for the optimally fluorine-doped and overdoped Hg1201 samples. In the optimally doped compound, the fluorine atoms occupy the position (1/2, 1/2, 0). An increase in the fluorine content leads to the partial replacement of oxygen atoms in the position (0, 0, ~0.21) with fluorine atoms (in the axial vertex of the CuO_6 octahedron).[67] The structures of the optimum fluorine-doped (T_c = 97 K) and overdoped ($T_c \approx$ 80 K) compounds were

refined by the powder neutron-diffraction method. The refined occupancies of the anion position (1/2, 1/2, 0) in the mercury-containing layer are 0.24(2) and 0.32(2) for two compounds, respectively. These values are substantially larger than the occupancies found for the oxygen-oxidised Hg1201 phases with the similar temperatures T_c [0.124(9) and 0.19(1), respectively].[68] The plots of T_c *versus* the fluorine or oxygen content in the mercury-containing layer are dome-shaped. However, the curve for the fluorinated samples is shifted toward larger δ values (Fig. 9). As is evident from Fig. 9, twice as much fluorine as compared to that of oxygen is required for the same T_c values and the corresponding doping level to be attained, which corresponds to the difference in the formal charges of the O^{2-} and F^- anions. This fact provides support for the ionic model of doping of mercury-containing cuprates, *viz*., an oxygen atom creates twice as many holes in the conduction band as that generated by a fluorine atom.

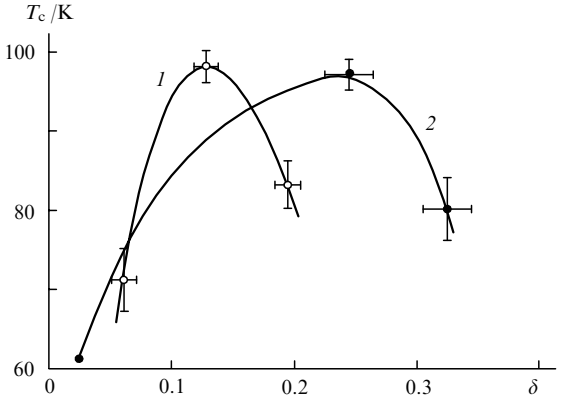


Figure 9. Plot of T_c *vs*. the excessive oxygen (*1*) or fluorine (*2*) contents in the Hg1201 phase.

The dependence of T_c on the unit cell parameter a (or on the interatomic $Cu-O_{eq}$ distance in the plane of the CuO_2 layer) both for the fluorinated and oxygen-oxidised samples can be approximated by a single parabolic curve with a maximum at 97 K and $a = 3.882$ Å (Fig. 10). Hence, the same superconducting transition temperatures in complex mercury-containing cuprates can be achieved not only at the same doping level but also with approximately equal equatorial $Cu-O_{eq}$ bond lengths. If the oxidation state of copper remains constant, the $Cu-O_{eq}$ distances are virtually independent of the amount of hyperstoichiometric anions. In contrast, the $Cu-O_{ax}$ distance changes substantially as the occupancy of the anion position in the mercury-containing layer is varied, *viz*., the $Cu-O_{ax}$ bond is shortened as the amount

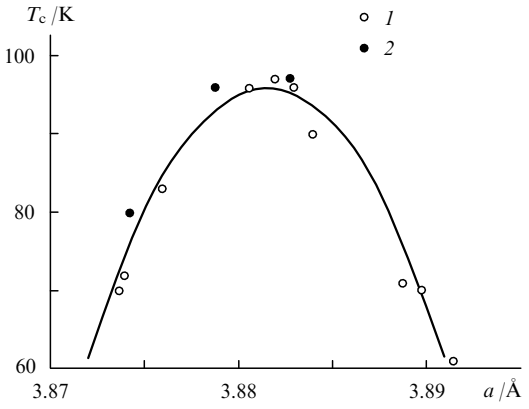


Figure 10. Plot of T_c *vs*. the unit cell parameter a for oxygen-doped (*1*) and fluorinated (*2*) Hg1201 samples.

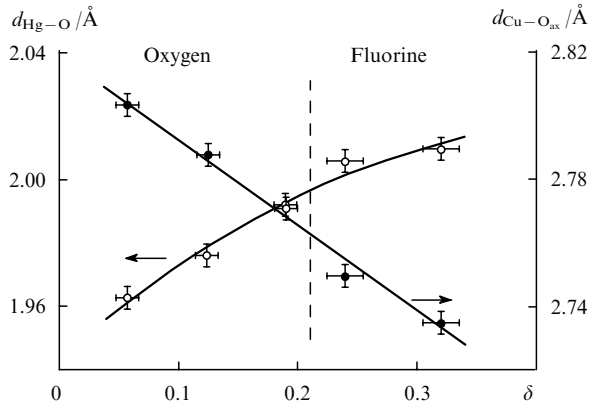


Figure 11. Interatomic $Cu-O_{ax}$ and $Hg-O$ distances *vs*. the amounts of the oxygen or fluorine atoms in the mercury-containing layer.

of the hyperstoichiometric anions is increased. Figure 11 shows the virtually linear dependence of this distance on the amount of excessive (δ) oxygen or fluorine. In the fluorinated compounds, this bond is substantially shorter than those in oxygen-containing compounds with similar T_c.

Apparently, shortening of the $Cu-O_{ax}$ distances results from extension of the $Hg-O$ dumbbells, which is associated with an increase in the coordination number of the mercury atoms due to incorporation of additional anions in the mercury-containing layer. This leads to the displacement of the O_{ax} atom from mercury to copper accompanied by a noticeable shortening of the $Cu-O_{ax}$ distance, the $Cu-O_{eq}$ bond lengths and T_c remaining virtually constant. This change in the interatomic distances can be considered to be a result of anisotropic contraction of the CuO_6 octahedra under the action of the external pressure (~ 2 GPa) applied along the c axis.[69] According to $dT_c/dP \approx 2$ K GPa^{-1} for the optimally oxygen-doped compound,[70] T_c for the fluorinated sample with $\delta_F \approx \delta_{opt}$ would be expected to increase by ~ 4 K. The fact that the optimally fluorine- and oxygen-doped samples have identical T_c indicates that shortening of the $Cu-O_{ax}$ bond exerts only a slight effect on the increase in T_c in mercury-containing cuprates under the influence of the applied external pressure. The increase in T_c is most probably caused by shortening of the $Cu-O_{eq}$ distances.

This conclusion was confirmed by the results of studies of the fluorinated $Hg_{0.8}Ba_2Ca_2Cu_{3.2}O_{8+\delta}$ samples (Hg1223 phase). The reduced Hg1223 sample ($T_c = 100$ K) was divided into two portions one of which was annealed under a stream of oxygen, and the remaining portion was fluorinated. For both samples, T_c was found to be increased, but the transition temperature for the fluorinated sample was 4 K higher (138 K) than that for the oxygen-oxidised sample (134 K).[71,72] The unit cell parameters a and c of these samples are given below:

Sample	a /Å	c /Å
$Hg_{0.8}Ba_2Ca_2Cu_{3.2}O_{8+\delta}$	3.8524(4)	15.819(4)
$Hg_{0.8}Ba_2Ca_2Cu_{3.2}O_8F_{2\delta}$	3.8501(2)	15.773(3)

The structure of the fluorinated sample was refined based on the neutron diffraction data.[72] In this sample, two anion positions in the mercury-containing layer, *viz*., (1/2, 1/2, 0) and (1/2, 0, 0), are occupied with occupancies of 27(1)% and 10(1)%, respectively, as distinct from the fluorinated Hg1201 sample. Apparently, the fact that the anions occupy the position (1/2, 0, 0) is associated with the partial replacement of the mercury atoms with copper atoms. The total amount of anions in the mercury-containing layer of the fluorinated sample with the maximum T_c value is substantially larger than the amount of hyperstoichiometric oxygen in the optimally oxygen-doped sample [18% and 8% for the positions (1/2, 1/2, 0) and (1/2, 0, 0), respectively].[73]

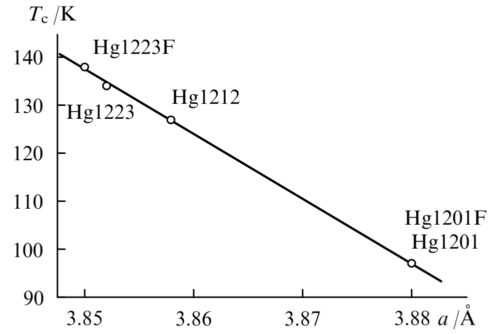


Figure 12. Maximum T_c *vs.* the unit cell parameter a for oxygen-oxidised and fluorinated mercury-containing cuprates.

The maximum T_c values for the first three members of the homologous series of mercury-containing complex cuprates $HgBa_2Ca_{n-1}Cu_nO_{2n+2+\delta}$ and the fluorinated Hg1201 and Hg1223 phases depend linearly on the unit cell parameter a; $dT_c/da \approx 1350$ K Å^{-1} (Fig. 12).[72,74] It is believed that the T_c for these compounds depends on the degree of contraction of the CuO_2 planes induced by the modification of the chemical composition. The similar value of dT_c/da was also found upon epitaxial contraction of thin single-crystalline films of $La_{0.9}Sr_{0.1}CuO_4$.[75]

For the fluorinated Hg1223 sample, the absolute value of dT_c/da is almost an order of magnitude larger than dT_c/da obtained under the applied external pressure ($dT_c/dP \approx$ 1.7 K GPa^{-1}, $dT_c/da \approx -160$ K Å^{-1}).[76] This difference may be attributed to the structural changes of the CuO_2 layers. In the Hg1201 phase, these layers are planar, whereas the Cu–O–Cu angle in the Hg1212 phase is close to 180°.[77] High external pressure causes corrugation of the CuO_2 layers. For example, the Cu–O–Cu angle in the Hg1223 structure is decreased to 175.0° at a pressure of 2 GPa, T_c being increased to 138 K. The Cu–O–Cu angle in the Hg 1223 phase changes only slightly upon fluorination (178.4° and 177.3° for the oxidised[77] and fluorinated samples, respectively). The Cu–O–Cu bond angle is an important parameter governing T_c. For HTSC with $T_c > 100$ K, the deviation of this angle from 180° is no larger than 4°.

Hence, chemical modifications of the structure, which lead to a decrease in the Cu–O distance without a change in the degree of corrugation of the CuO_2 layers, is a promising way of increasing T_c in complex superconducting copper oxides.

3. Fluorine incorporation into structures of non-superconducting anion-deficient perovskite-like complex cuprates

Let us discuss the effect of fluorine incorporation on the structure and properties of anion-deficient copper-containing perovskites, which do not exhibit superconducting properties but which, nevertheless, could become superconductors if the appropriate doping level is achieved and the compound attains a structure suitable for the manifestation of superconductivity.

Perovskite-like complex cuprates with structures of brownmillerite $MACuGaO_5$ (M = La, Pr or Nd; A = Ca or Sr), which are denoted as Ga1201,[49,50] belong to the orthorhombic system (Fig. 13 *a*) with the parameters $a \approx 4a_p, b \approx c \approx a_p\sqrt{2}$ (a_p is the parameter of the perovskite sublattice) and consist of alternating layers

$$-CuO_2-M_{0.5}A_{0.5}O-GaO\square-M_{0.5}A_{0.5}O-CuO_2-$$
$$\longleftarrow a/2 \longrightarrow$$

The gallium and copper cations are in the tetrahedral and octahedral coordination environments, respectively. The GaO_4 tetrahedra in the plane of the GaO□ layer share vertices to form chains along the c axis of the unit cell. The ordered arrangement of the oxygen atoms and anion vacancies in these layers leads to distortion of the equatorial coordination environment about the copper atoms. In the Ga1201 compounds, two short (1.89 Å) and two long (1.96 Å) Cu–O distances were found.[78,79] The substantial difference in the $Cu-O_{eq}$ bond lengths in the plane of the CuO_2 layers may be responsible for the fact that these compounds do not exhibit superconducting properties even if the appropriate oxidation state of copper is achieved. Actually, the $La_{1-x}Sr_{1+x}CuGaO_5$ solid solution (Ga1201 phase) ($0 \leqslant x \leqslant 1.2$, the maximum oxidation state of copper is +2.2) are not superconductors.[80] At the same time, homologues of the Ga1201 compounds, *viz*., the Ga1212 compounds, possess superconducting properties. This difference in the properties is associated with the difference in the coordination environment of the copper atoms in these compounds. In the structure of the superconductor $Y_{0.6}Ca_{0.4}Sr_2Cu_2GaO_7$ (T_c = 44 K), the copper atoms occupy the centres of the square pyramids formed by the oxygen atoms, the equatorial Cu–O distances being virtually equal (1.92 and 1.93 Å).[51]

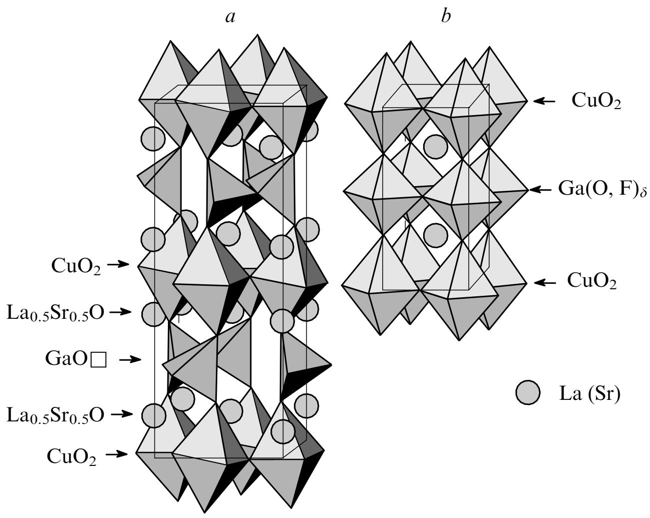


Figure 13. Crystal structures of $LaSrCuGaO_5$ (*a*) and $LaSrCuGaO_{5-x}F_{2x-\delta}$ (*b*).

For the Ga1201 phases to exhibit superconducting properties, not only the appropriate doping level must be achieved but also strong distortion of the structure caused by the anion ordering in the GaO□ layers must be diminished. This can be attained by inserting fluorine atoms into the anion vacancies. In this case, an increase in the formal oxidation state of copper will be accompanied by the formation of the five- and six-coordinate environment about the gallium atoms, which is favourable for a depression of the orthorhombic distortion and equalisation of the equatorial Cu–O distances.

The treatment of $LaACuGaO_5$ (A = Ca, Sr) with xenon difluoride led to a decrease in distortion of the unit cell up to the transition of the orthorhombic phase into the tetragonal phase (for A = Sr) with the parameters $a \approx a_p$, $c \approx 2a_p$.[81] Upon fluorination, the oxidation state of copper depends substantially on the reaction conditions. If fluorination is carried out over a long period (150 h) in the presence of a large excess of xenon difluoride at rather low temperature (573 K), the reaction proceeds according to the combined mechanism of anion exchange and fluorine incorporation:

$$LaSrCuGaO_5 + (x + y/2)\,XeF_2 \longrightarrow$$
$$\longrightarrow LaSrCuGaO_{5-x}F_{2x+y} + x\,[O] + (x + y/2)\,Xe.$$

Upon such fluorination, the oxidation state of copper reaches +2.16. An elevation of the temperature to 673 K is accompanied by a slight reduction in the oxidation state of copper (to +1.95)

due to the fact that the anion exchange becomes the predominant process:

$$LaSrCuGaO_5 + (x - \delta/2)\,XeF_2 \longrightarrow$$
$$\longrightarrow LaSrCuGaO_{5-x}F_{2x-\delta} + x[O] + (x - \delta/2)\,Xe.$$

The result of structural transformation occurring upon fluorination is shown in Fig. 13 *b*. Excessive fluorine atoms partially occupy the vacancies in the $GaO\square$ layers and the coordination environment about the gallium atoms becomes nearly octahedral. The oxygen and fluorine atoms and the anion vacancies are arranged in a disordered fashion in the positions (1/2, 0, 1/2). In the case of the space group *P*4/*mmm* and the above-mentioned unit cell parameters, the CuO_2 layers must be planar and the Cu–O distances in the plane of the layer must be equal in length. In such a situation, the structure of the fluorinated phase will meet the criteria necessary for the manifestation of superconducting properties. However, all attempts to perform the transition of fluorinated samples into the superconducting state failed whatever the doping level used.

The simplest copper oxyfluorides which can exhibit superconducting properties are hypothetical solid solutions with composition $(La,Sr)CuO_2F$ based on the perovskite structure. The required oxidation state of copper can be achieved through the heterovalent replacement of La with Sr in the A sublattice. These solid solutions must have a structure of tetragonally distorted perovskite containing CuO_2 planar layers and fluorine atoms in the axial positions of the octahedra about the copper atoms. These compounds can be synthesised by soft fluorination of anion-deficient perovskites in the ratio (La,Sr)/Cu = 1.

Various perovskite-like anion-deficient copper oxides are known whose three-dimensional structures differ primarily by the character of ordering of the oxygen atoms and anion vacancies within the *ab* plane of the perovskite sublattice. Thus, the columns of the oxygen atoms passing along the [001] direction are removed in a certain order resulting in a decrease in the coordination number of the copper atoms from 6 to 5, 4 or 2. Among these oxides are also the $(La_{1-x}Sr_x)_8Cu_8O_{20-\delta}$ solid solutions with tetragonal structures and the unit cell parameters $a \approx a_p2\sqrt{2}$, $c \approx a_p$ (Fig. 14).[82, 83]

For a superconducting compound to be prepared, the character of the distribution of the oxygen atoms in the starting compound must be changed upon fluorination so as to form the CuO_2 planes. Fluorination of $La_{6.5}Sr_{1.5}Cu_8O_{19.65}$ with xenon difluoride afforded a tetragonal perovskite-like phase with the presumed composition $La_{0.813}Sr_{0.187}Cu(O,F)_{3-\delta}$ and the unit cell parameters $a < c \approx a_p$.[84] In a single sample, the fluorinated phase always coexists with the starting phase within one crystallite (Fig. 15). Thermal treatment at 673 K in air led to decomposition of $La_{0.813}Sr_{0.187}Cu(O,F)_{3-\delta}$ to give LaOF and SrF_2, which indicates that this phase contains a substantial amount of fluorine. The structure of $La_{0.813}Sr_{0.187}Cu(O,F)_{3-\delta}$ was refined by the Rietveld method and confirmed by HRTEM (see Fig. 14). In the structure of this compound, the anion positions in the equatorial environment about the copper atoms are completely occupied, whereas the vacancies are located in the axial positions. The Jahn–Teller effect induced by an octahedral coordination about some copper atoms causes elongation of the axial distances (2.026 Å) as compared to the equatorial distances (1.896 Å) and the tetragonal distortion of the perovskite unit cell. Oxyfluoride $La_{0.813}Sr_{0.187}Cu(O,F)_{3-\delta}$ does not exhibit superconducting properties.

The two examples considered above show that filling of the anion vacancies upon fluorination diminishes structural distortions caused by the ordering of the oxygen vacancies. However, the statistical distribution of the fluorine and oxygen atoms and the anion vacancies over certain crystallographic positions [for example, in the equatorial environment about the gallium atoms in the structures of fluorinated brownmillerites or in the axial positions of the $Cu(O,F)_{6-\delta}$ octahedra in the $La_{0.813}Sr_{0.187}$.

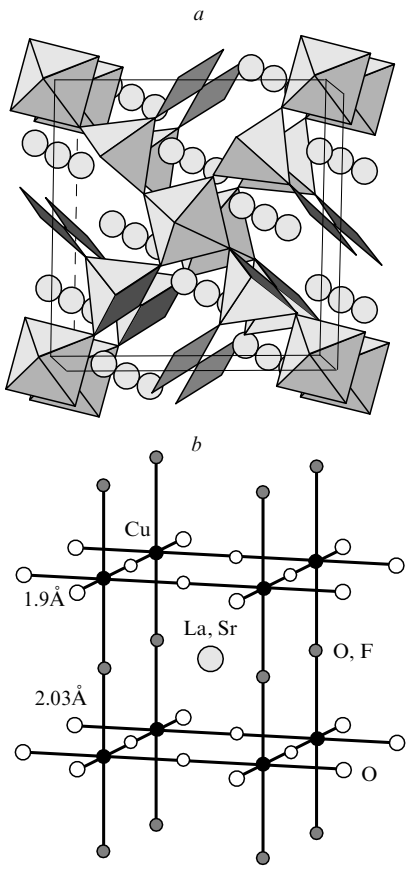


Figure 14. Scheme of the structural transformations of $La_{6.5}Sr_{1.5}.Cu_8O_{19.65}$ (*a*) into $La_{0.813}Sr_{0.187}Cu(O,F)_{3-\delta}$ (*b*) upon fluorination.

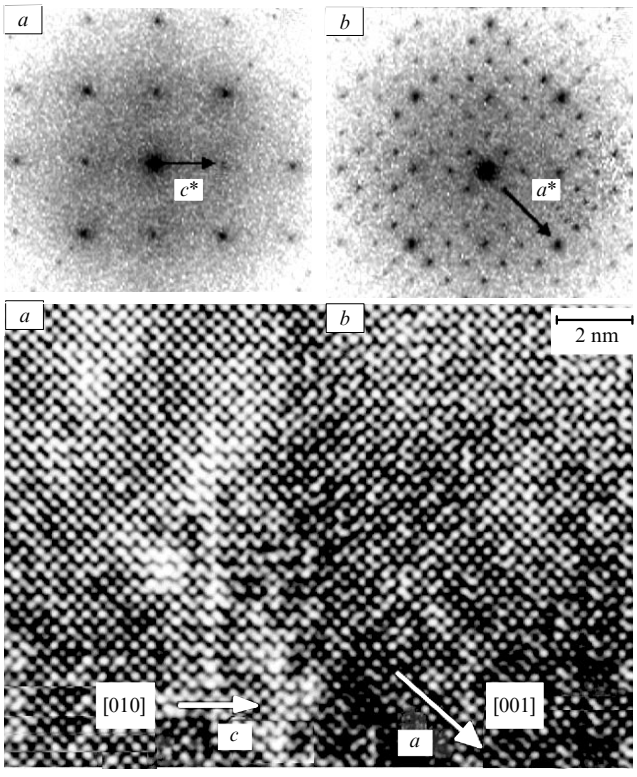


Figure 15. HRTEM images of the domains of the fluorinated $La_{0.813}Sr_{0.187}Cu(O,F)_{3-\delta}$ (*a*) and starting $La_{6.5}Sr_{1.5}Cu_8O_{19.65}$ (*b*) phases. In the optical diffraction patterns, suppression of the superstructure with $a_p2\sqrt{2}$ upon fluorination is shown.

.$Cu(O,F)_{3-\delta}$ structure] may be responsible for substantial static displacements (associated with the presence of the B-type cations possessing non-completed coordination spheres) and, as a consequence, can cause local distortions of the CuO_2 layers. This fact as well as the possibility of the partial replacement of oxygen with fluorine in the CuO_2 layers may account for the fact that fluorinated anion-deficient perovskite-like cuprates do not show superconductivity.

4. Incorporation of fluorine atoms into interlayer cavities in the structures of complex cuprates

Fluorination of anion-deficient cuprates is most often accompanied by the formation of compounds with simpler high-symmetry structures, whereas fluorination of complex copper oxides with the filled anion sublattice leads most commonly to structural distortions. The $(M',M'',A)_2CuO_{4-\delta}$ compounds (M′ and M″ are rare-earth cations of different radii, A is an alkaline-earth cation) have structures with ordered alternation of the CuO_2 layers and the $(M,A)_2O_2$ blocks. These structures contain interlayer cavities accessible to additional anions. These cuprates crystallise in three structural types, *viz.*, *T*, *T*′ and *T**. In the structures of the *T* phases [La_2CuO_4, $La_{2-x}A_xCuO_{4-\delta}$ (A = Sr or Ba), the K_2NiF_4 structural type], the CuO_2 layers alternate with the NaCl-type [(La,A)O][O(La,A)] blocks (Fig. 16). Rare-earth cuprates having smaller ionic radii (M = Pr–Gd) crystallise in the *T*′ type structure. The structures of the *T*′ phases can be represented as the result of alternation of the fluorite-like $(M)(O_2)(M)$ fragments (see Fig. 2) and the CuO_2 layers. The *T** phases [$(La,M,Sr)_2$. .$CuO_{4-\delta}$, M = Sm–Er] contain both types of blocks, *viz.*, fluorite- and NaCl-like blocks, so that the structures of these phases can be described as the following sequence of layers:

$$-CuO_2-(La,Sr)O-O(La,Sr)-CuO_2-M,La-O_2-M,La-CuO_2-.$$

In all three structural types, the cations occupy the same positions, but these structural types differ in the distributions of the anions in the $(M,A)_2O_2$ blocks. If it is considered that the cations form a close packed motif, the NaCl-type [(M,A)O)(O(M,A)] block in the *T* phases is formed by the arrangement of the oxygen atoms in the octahedral cavities of the close packing. In the structures of the *T*′ phases, the fluorite-like $(M)(O_2)(M)$ block is formed by the arrangement of the oxygen atoms in half of the tetrahedral cavities. Hence, the anion positions in the $(M,A)_2O_2$ blocks, which are occupied by the oxygen atoms in the *T* phase, remain vacant in the *T*′ phase and *vice versa* (see Fig. 16). Additional anions in the structures of this type are located in vacant interlayer tetrahedral (in the case of the NaCl-like blocks) or octahedral (in the case of the fluorite-like blocks) cavities. When both types of cavities are simultaneously occupied, the distances between the anions in the $(M,A)_2O_2$ block and the anions in the interlayer cavities are no larger than 2–2.15 Å. The arrangement of like-charged ions at such short distances will destabilise the structure and it can be substantially distorted due to Coulombic repulsions between the anions.

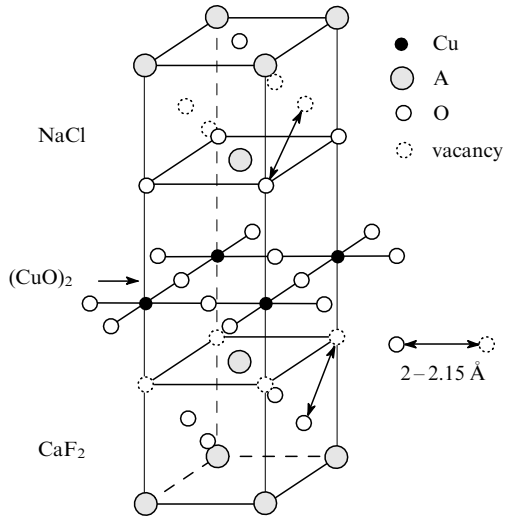
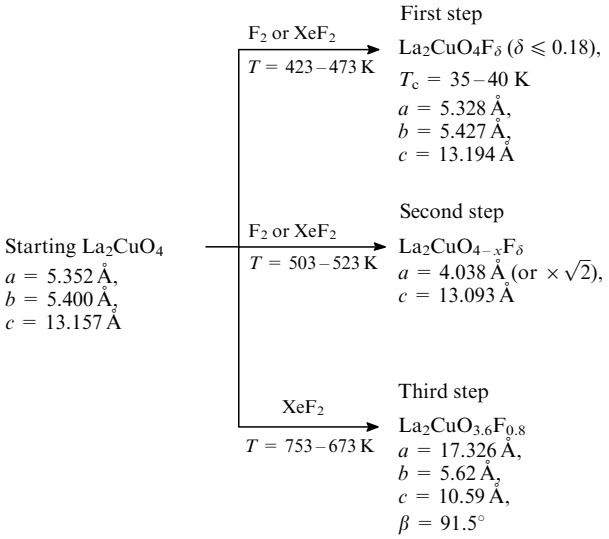


Figure 16. Scheme of formation of the intergrowth structures with alternation of CuO_2 layers and the fluorite- and/or NaCl-type $(M,A)_2O_2$ blocks.

Lanthanum cuprate La_2CuO_4 was one of the first compounds that was subjected to fluorination to obtain a superconductor.[24,27,30,85–87] Fluorination of this cuprate with various agents gave rise to oxyfluorides, which differ in the structure and properties depending on the conditions of thermal treatment. The main steps of the incorporation of fluorine into La_2CuO_4 are shown in Scheme 1.

Scheme 1



The treatment of La_2CuO_4 with fluorine or XeF_2 at a rather low temperature afforded fluorinated lanthanum cuprate with T_c = 35–40 K. The incorporation of small amounts of fluorine ($\delta \leqslant 0.18$) into the La_2CuO_4 structure is accompanied by an increase in the degree of orthorhombic distortion of the unit cell and an insignificant increase in the parameter *c*.[27] Neutron diffraction studies of the crystal structures of the starting and fluorinated samples demonstrated that low degrees of fluorination do not cause substantial rearrangements of the initial structure.[85] Excessive fluorine atoms are located in the interlayer cavities, which are tetrahedrally surrounded by the lanthanum atoms (NaCl-type block). The incorporation of fluorine atoms occurs analogously to that of oxygen atoms[88] and the degree of orthorhombic distortion, which depends on the amount of hyperstoichiometric anions, appeared to be similar for the oxygen-oxidised and fluorinated samples with similar anionic stoichiometry (a = 5.332 Å, b = 5.423 Å, c = 13.222 Å for $La_2CuO_{4.18}$).[89] Fluorination of the *T* phases in which lanthanum atoms are partially replaced with alkaline-earth metals gives rise to compounds exhibiting the superconducting properties at small degrees of replacement analogous to the effect of oxygen incorporation. Superconductivity was observed in the fluorinated solid solutions $La_{2-x}Sr_xCuO_4$ ($x < 0.1$, T_c = 36–40 K)[85,90] and $La_{2-x}Ba_x$. .CuO_4 ($x < 0.15$, T_c = 32–42 K).[86,91] In the case of higher strontium or barium contents, T_c for the initial and fluorinated samples remains identical.

The treatment of La_2CuO_4 with fluorine or XeF_2 at higher temperatures (503–523 K, the second step) gives rise to non-superconducting oxyfluoride with the body-centred tetragonal unit cell, which either corresponds to the K_2NiF_4 subcell[87] or differs from this subcell only by the parameter a equal to $\sqrt{2}a_{K_2NiF_4}$ ($a_{K_2NiF_4}$ is the unit cell parameter of K_2NiF_4).[92] In this step, the unit cell is substantially expanded in the *ab* plane

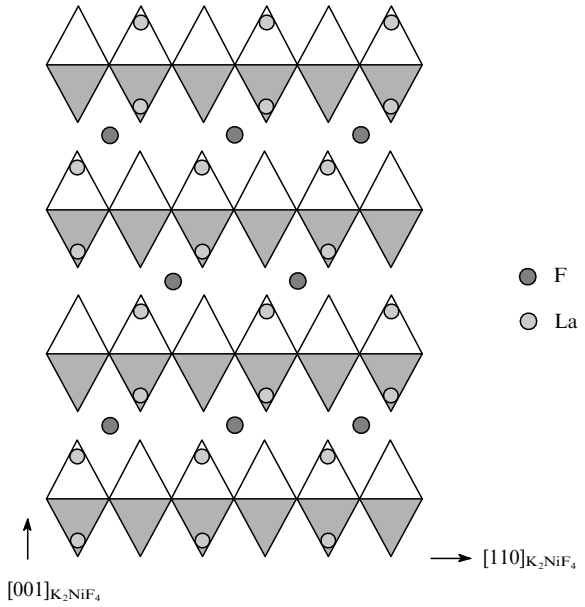


Figure 17. Model of the crystal structure of oxyfluoride formed upon fluorination of La_2CuO_4 at 523 K. The copper atoms are in an octahedral environment.

($a_{K_2NiF_4} = a/\sqrt{2} \approx 3.802$ Å and $a_{K_2NiF_4} = 4.038$ Å for the initial and fluorinated samples, respectively). Electron diffraction studies revealed a superstructure with $a = 2\,a_{K_2NiF_4}$, $c = 2c_{K_2NiF_4}$ (see Ref. 87) formed due to the alternation of the vacant and occupied tetrahedral cavities along the $[001]_{K_2NiF_4}$ and $[110]_{K_2NiF_4}$ directions (Fig. 17). This ordering may also be accompanied by cooperative rotation of the CuO_6 octahedra about the $[\bar{1}10]_{K_2NiF_4}$ direction to achieve the maximum distances between the oxygen atoms involved in the axial environment about the copper atoms and the anions in the interlayer cavities.

In the third step, the interaction with XeF_2 proceeds predominantly through a mechanism of anion exchange to give oxyfluoride with composition $La_2CuO_{3.6}F_{0.8}$ containing copper in the oxidation state +2. This compound belongs to the monoclinic system and its unit cell is determined by the following vectors:[87]

$$\mathbf{a}_m = 2(\mathbf{a}_{K_2NiF_4} + \mathbf{b}_{K_2NiF_4}) + \mathbf{c}_{K_2NiF_4},$$

$$\mathbf{b}_m = -\mathbf{a}_{K_2NiF_4} + \mathbf{b}_{K_2NiF_4},$$

$$\mathbf{c}_m = -\frac{1}{2}(3\mathbf{a}_{K_2NiF_4} + 3\mathbf{b}_{K_2NiF_4} - \mathbf{c}_{K_2NiF_4}),$$

$$\beta \approx 91.5^\circ.$$

The structural model established based on the results of a electron diffraction study and the HRTEM method is shown in Fig. 18. The fluorine atoms occupy 40% of the tetrahedral cavities in an ordered fashion. In this case, the oxygen atoms are partially removed from the LaO layers and a part of the CuO_6 octahedra are transformed into the CuO_5 square pyramids. The remaining octahedra are rotated about the b_m axis in such a way that the distances between the axial oxygen atoms and the fluorine atoms become lower. The blocks in which the tetrahedral positions are occupied and the axial oxygen atoms are removed (fluorite fragments) alternate with the NaCl-type fragments. However, the alternation of these blocks, unlike that observed in the T^* phases, occurs not only along the $[001]_{K_2NiF_4}$ direction but also along the $[110]_{K_2NiF_4}$ direction.

Lanthanum cuprate La_2CuO_4 can be considered as the first member of the homologous series of cuprates with structures of the Ruddlesden–Popper phases $(M,A)_{n+1}Cu_nO_{2n+2+\delta}$ (M = REE, A = Ca or Sr) with $n = 1$. The structure of the

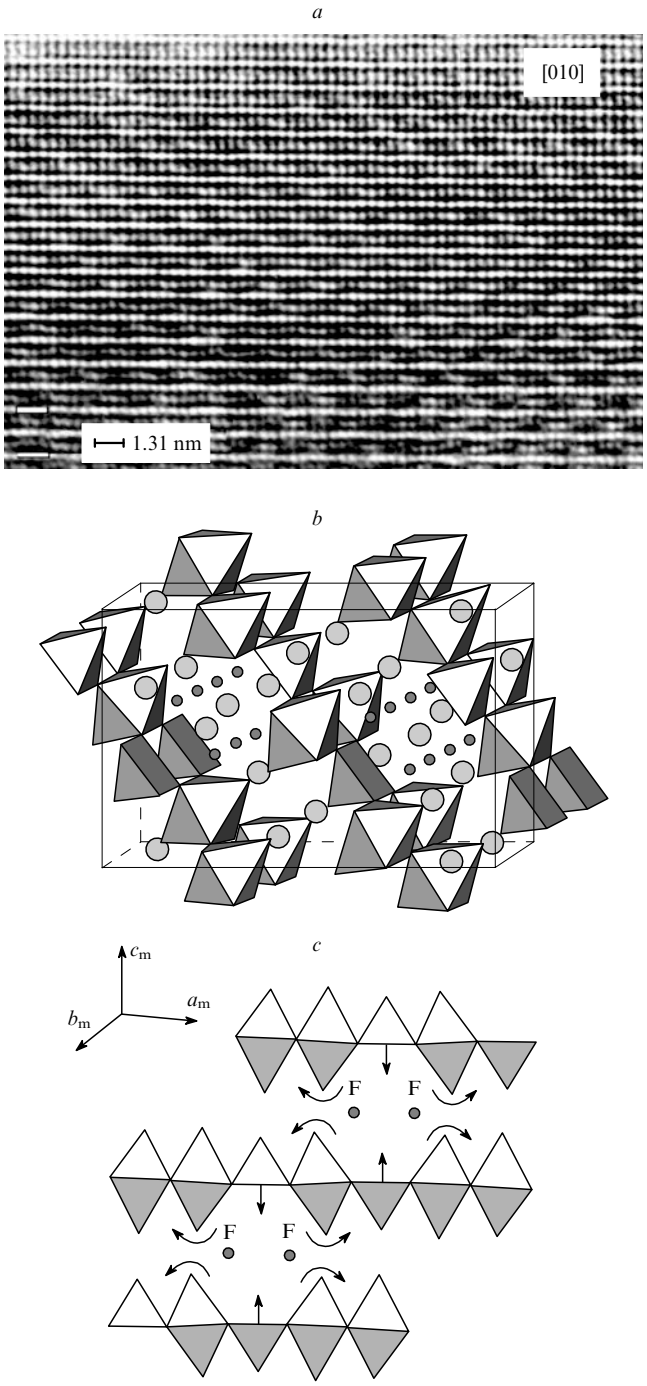


Figure 18. HRTEM images (*a*), the structural model (the copper atoms are in the octahedra and tetragonal pyramids) (*b*) and the projection displaying the directions of cooperative atomic displacements in the $La_2CuO_{3.6}F_{0.8}$ phase (*c*).

homologue with $n = 2$ ($M_{2-x}A_{1+x}Cu_2O_{6+\delta}$) contains doubled CuO_2 layers separated by A□ layers:

$$-CuO_2-O(M,A)-(M,A)O-CuO_2-A\square-CuO_2-(M,A)O-$$

$$-O(M,A)-CuO_2-,$$

the cation positions in the A□ layer can be occupied simultaneously by rare-earth and alkaline-earth atoms as, for example, in the case of A = Sr (Fig. 19). In this compound, the copper atoms have a square-pyramidal coordination. This structure, unlike the structure of the preceding member of the homologous series, contains two possible positions suitable for location of additional

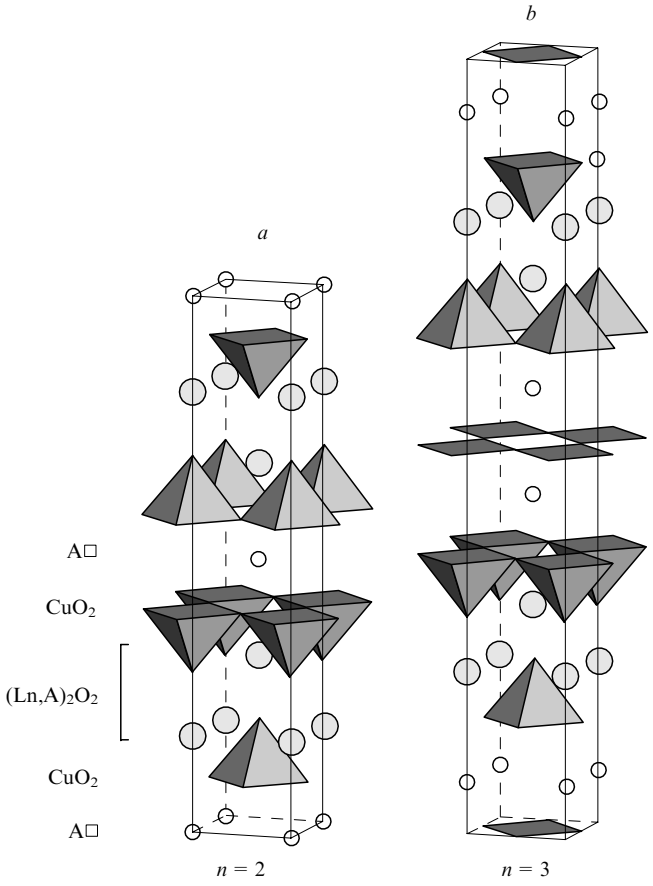


Figure 19. Crystal structures of the members of the homologous Ruddlesden – Popper series with $n = 2$ (*a*), 3 (*b*).

anions, *viz*., in tetrahedral cavities of the $(Ln,A)_2O_2$ block and in the A□ layer with completion of the coordination environment about copper to an octahedron.

The behaviour of these compounds upon fluorination differs from that of La_2CuO_4. The treatment of $La_{1.9}Sr_{1.1}Cu_2O_{6.05}$ and $La_{1.9}Ca_{1.1}Cu_2O_{5.95}$ with reagents, such as F_2, NH_4F or CuF_2, led initially to an increase in the parameters *a* and *c* of the tetragonal unit cell. However, further increase in the degree of fluorination caused the transformation of the Sr-containing sample into the orthorhombic phase accompanied by a decrease in the unit cell parameters in the *ab* plane and a substantial increase in the parameter *c* (from 20.048 to 21.68 Å).[25] The authors of the cited study [25] related the formation of the orthorhombic phase characterised by the larger parameter *c* (and, correspondingly, by the larger distance between the CuO_2 layers) to the facts that the positions in the A□ layer are occupied by fluorine atoms and some copper atoms have an octahedral environment. For $La_{1.9}Ca_{1.1}Cu_2O_{5.95}$, this effect was not observed due, apparently, to the smaller distance between the CuO_2 layers because the calcium atom is smaller than the strontium atom.

Superconducting oxyfluorides of this series with $n = 2$, 3 were synthesised at high pressure. Samples with compositions $Sr_2CaCu_2O_{4.6}F_2$ and $Sr_2Ca_2Cu_3O_{6.2}F_{3.2}$ showed bulk superconductivity ($T_c = 99$ and 111 K, respectively) in spite of the fact that they contained substantial amounts of impurity phases.[11] The $Sr_2NdCu_2O_5F$ compound turned out to be single-phase and did not exhibit superconducting properties because it contained copper in the oxidation state +2. However, the $Sr_2Nd_{0.2}.Ca_{0.8}Cu_2O_5F$ solid solution generated upon the partial replacement of neodymium with calcium showed the superconducting transition at 85 K.[9] It was suggested that the fluorine atoms in all these phases are located in the NaCl-type blocks and are involved in the (SrF)(FSr) or $(SrO_{0.5}F_{0.5})(F_{0.5}O_{0.5}Sr)$ layers. The crystal structures of superconducting complex copper oxyhalides belonging to the Ruddlesden – Popper phases have been surveyed in the review.[93]

Of complex copper oxyfluorides, fluorine derivatives of Nd_2CuO_4 have received the most study. Most of the investigations were devoted to the structures and properties of the $Nd_2CuO_{4-x}F_x$ solid solutions in which the *n*-type superconductivity with $T_c = 27$ K (at $x = 0.3$) was revealed.[3] As mentioned above (see Section III), the partial replacement of oxygen atoms in the fluorite-like Nd_2O_2 blocks with an equivalent amount of fluorine has virtually no effect on the crystal structure of the resulting compound. Fluorine incorporation into the Nd_2CuO_4 structure afforded a new phase with composition $Nd_2CuO_3F_2$.[94] This compound was found by electron microscopy in samples prepared by fluorination of Nd_2CuO_4 with xenon difluoride at 573 – 673 K. This phase crystallises in the monoclinic system (the unit cell parameters $a \approx 12.96$, $b \approx 5.5$, $c \approx 5.8$ Å, $\beta \approx 92°$). The model structure of this compound was constructed from images obtained by the HRTEM method. According to this model, a portion of the anions which are located in the positions tetrahedrally coordinated by the neodymium atoms form chains along the *c* axis alternating with chains of the vacancies along the *b* direction (Fig. 20). Another portion of anions occupy axial positions in the octahedral environment about the copper atoms. The presence of copper atoms possessing octahedral coordination is responsible for the increase in the parameter *c* from 12.167 in the starting phase to 12.96 Å in the fluorinated compound. The layers of the $Cu(O,F)_6$ octahedra are distorted due to the cooperative rotation required for the maximum distance between the anions to be attained.

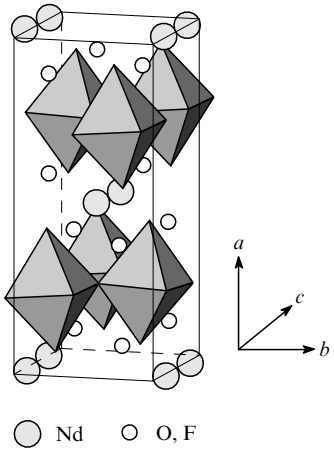


Figure 20. Crystal structure of $Nd_2CuO_3F_2$.

The $Nd_2CuO_3F_2$ compound is structurally similar to $La_2CuO_{3.6}F_{0.8}$. The structures of these compounds are analogous to the structure of the T^* phase and can be considered as intermediate between the structures of the *T* and T' phases. In both structures, the NaCl- and fluorite-like blocks alternate not only along the *c* axis of the tetragonal subcell but also in the *ab* plane. In both cases, the ratios between the parameters of the tetragonal subcells $c/3a \approx 1.08$ are in the T^*-phase stable region ($c/3a \approx 1.15$ for *T* phases, $c/3a \approx 1.06 - 1.08$ for T^* phases and $c/3a \approx 1.02$ for T' phases [95]).

Apparently, the results of fluorination of the T^* phases depend substantially on their cation composition. The refinement of the crystal structures of $La_{1.25}Dy_{0.75}CuO_{3.75}F_{0.5}$ (see Ref. 34) and $LaBa_{0.2}Gd_{0.8}CuO_{3.55}F_{0.8}$,[96] which were prepared by fluorination of the corresponding cuprates with ZnF_2 and CuF_2, demonstrated that excessive anions were located in the tetrahedral cavities of the NaCl-type blocks, while the fluorite-like blocks remained unchanged. Repulsions between the anions and/or a

reduction in the formal oxidation state of copper lead to elongation of the equatorial Cu–O distances from 1.933 to 1.942–1.962 Å as well as to a small increase in the parameter *c*. However, the $LaBa_{0.2}Gd_{0.8}CuO_{3.55}F_{0.8}$ structure retains tetragonal symmetry, whereas $La_{1.25}Dy_{0.75}CuO_{3.75}F_{0.5}$ crystallises in the orthorhombic system with the unit cell parameters *a* and *b*, which are increased by a factor of $\sqrt{2}$. In both cases, the atoms occupying the axial vertices in the $Cu(O,F)_5$ pyramids are shifted from the ideal positions in the *ab* plane due, probably, to their interactions with the anions located in the interlayer cavities.

Samples prepared by fluorination of the *T** phase $LaHo_{0.75}Sr_{0.25}CuO_{3.9}$ with xenon difluoride have complex microstructures, which can be described as narrow extended domains of a phase with high fluorine content (phase I) located in a matrix of the low-fluorinated orthorhombic *T** phase (phase II) (Fig. 21).[97] The results of the HRTEM study demonstrated that the structure of the fluorite-like blocks in the low-fluorinated phase II remains unchanged, whereas the NaCl-type blocks acquire a structure similar to that of analogous blocks in $La_2CuO_{3.6}F_{0.8}$. Phase I belongs to the monoclinic system with the unit cell parameters $a_m \approx b_m \approx 5.5$ Å $\approx a_t\sqrt{2}$, $c_m \approx 12.84$ Å $\approx c_t$, $\beta \approx 91.4°$ (the subscripts m and t identify the monoclinic and tetragonal unit cells, respectively). As in the case of the *T*′ phase, an increase in the c_m parameter compared to $c_t = 12.553$ Å is indicative of the incorporation of additional anions into the axial positions of the coordination environment about the copper atoms. The characteristic feature of phase I is the identical distribution of the anions over the tetrahedral and octahedral positions resulting from fluorination of the initially different blocks, *viz*., the NaCl-type $(La_{0.75}Sr_{0.25}O)(OLa_{0.75}Sr_{0.25})$ and the CaF_2-type $(La_{0.25}Ho_{0.75})O_2(La_{0.25}Ho_{0.75})$ blocks (see Fig. 21). Consequently, not only the NaCl-type blocks but also the fluorite-like blocks undergo structural changes in the high-fluorinated samples. In the phase I, the vacant and occupied tetrahedral positions alternate in a 'staggered' fashion. The monoclinic distortion of phase I results from displacements of the A cations caused by interactions with the ordered oxygen and fluorine atoms in the tetrahedral cavities.

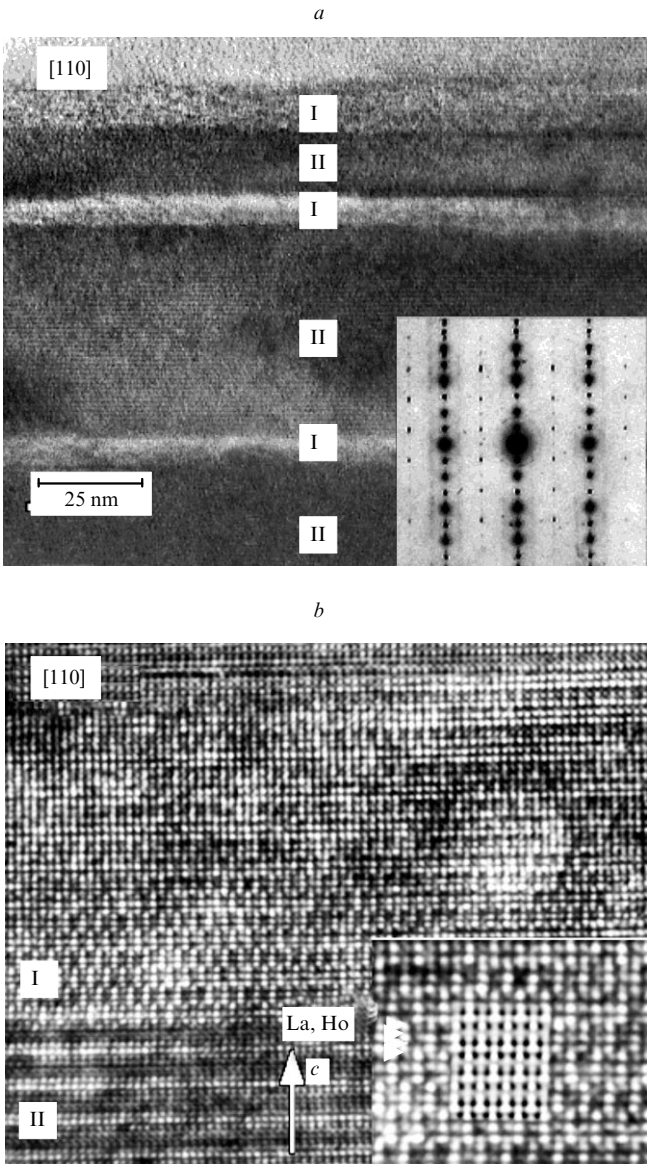


Figure 21. Electron microphotographs of the fluorinated $LaHo_{0.75}Sr_{0.25}CuO_{3.9}$ sample taken at a low magnification (*a*) and high resolution (*b*);[97] (*a*) the corresponding electron diffraction pattern is shown in the inset; (*b*) the inset presents an enlarged fragment of the image of phase I, which is superimposed on the theoretical image calculated from the proposed structural model; the $La_{0.25}Ho_{75}$ layers are indicated by arrows; I and II are phases with different fluorine contents.

Hence, the fluorine incorporation upon fluorination of the *T*, *T*′ and *T** phases has no direct effect on the CuO_2 planes, but these planes may be distorted due to cooperative rotation of the coordination polyhedra of the copper atoms. The $(M,A)_2O_2$ blocks are subjected to fluorination, the fluorine atoms first occupying the tetrahedral cavities in the NaCl-type blocks, while the fluorite-like blocks retain the initial structure under the same conditions. When two types of the anion positions are simultaneously occupied, these blocks undergo structural rearrangements, which are accompanied by the alternation of the NaCl- and fluorite-type structural fragments in directions perpendicular and parallel to the CuO_2 layers. Hence, the structures of the high-fluorinated compounds are intermediate between the structures of the *T* and *T*′ phases and are structurally similar to the *T** phases. A substantial increase in the parameter *c* for the fluorinated *T*′ and *T** phases occurs due to completion of the coordination polyhedron about the copper atom to a tetragonal pyramid or an octahedron.

In the fluorite- or NaCl-type $(M,A)_2O_2$ blocks in which the A positions are occupied by alkaline-earth and/or rare-earth cations, ionic interactions prevail. Because of this, the bonds in the (M,A)O layers in the NaCl-type blocks are comparable in strength to the bonds between the adjacent (M,A)O layers. The structures of Bi-containing layered cuprates $Bi_2Sr_2Ca_{n-1}Cu_nO_{2n+4+\delta}$ involve the NaCl-type Bi_2O_2 blocks. Unlike the $(M,A)_2O_2$ blocks containing isotropic chemical bonds, the BiO and OBi layers in the Bi_2O_2 block are linked only through van der Waals interactions, which is attributed to the crystal-chemical characteristics of the Bi^{3+} cation. Due to this structure of the Bi_2O_2 blocks, various halogen-containing agents (I_2, Br_2, $HgBr_2$ or LiI_3) can be intercalated into Bi-containing cuprates.[98–102] The iodine atoms intercalated into the Bi2212 and Bi2223 phases form an additional layer between the BiO and OBi layers as a result of which the distance between these layers is increased and the layers are shifted with respect to each other by a vector of the perovskite-like subcell (1/2, 1/2, 0) to form a primitive unit cell. After intercalation, the structural modulations of the BiO layers, which are characteristic of this family of superconductors due to the incommensurability of the Bi_2O_2 blocks and the CuO_2 layers, are retained because interactions between the intercalated atoms and the BiO and OBi layers are weak, the structures of the latter remaining virtually unchanged. In the compounds containing the intercalated F atoms, the Bi–F bond is more ionic than the bonds between the Bi atoms and other halogens and, hence, the results of incorporation of fluorine atoms into the structures of Bi-containing HTSC will be different.

Fluorination of $Bi_2Sr_{1.6}La_{0.4}CuO_{6.33}$ (Bi2201 phase, $T_c = 27$ K) with xenon difluoride led to an increase in the unit cell parameter *c* and was accompanied by suppression of the

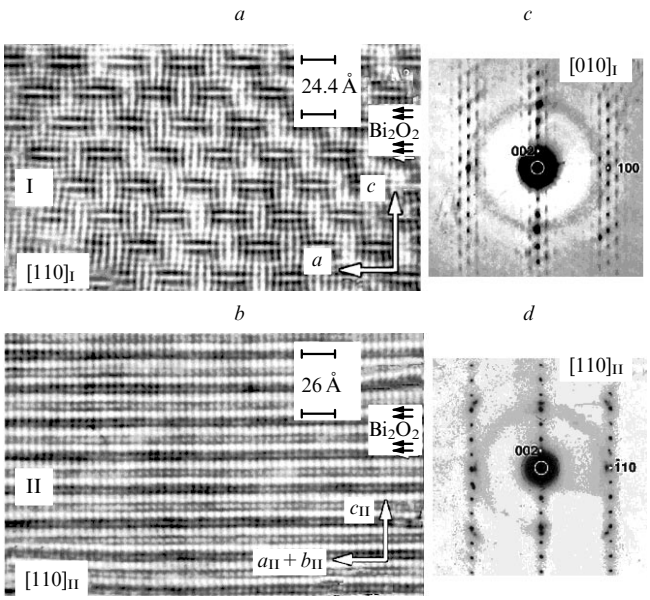


Figure 22. HRTEM images (*a*, *b*) and electron diffraction patterns (*c*, *d*) for the fluorinated Bi2201 phases of low (*a*, *c*) and high (*b*, *d*) fluorine contents.[103]
It can be seen that incommensurate modulations disappear as the degree of fluorination is increased.

superstructure $\sqrt{2}\,a_p \times \sqrt{2}\,a_p$ in the *ab* plane and the disappearance of the incommensurate modulations (Fig. 22), *i.e.*, by the formation of a tetragonal primitive unit cell with $a = 3.837$, $c = 26.18$ Å.[103] Consequently, the incorporated fluorine atoms change the structure of the BiO layers. Excessive anions occupy the cavities of the Bi_2O_2 blocks tetrahedrally coordinated by the Bi atoms so that the Bi_2O_2 blocks are transformed into the $Bi_2O_{2-x}F_{2+x}$ blocks in which the Bi atoms are located in monocapped square antiprisms to form short bonds with the F atoms and five long bonds with the O atoms (Fig. 23).

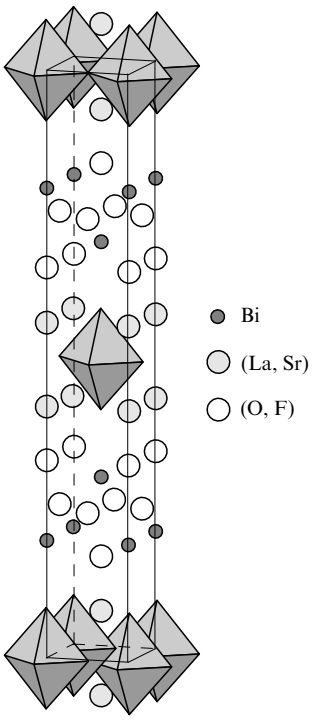


Figure 23. Crystal structure of the fluorinated Bi2201 phase.

Structurally analogous blocks were found in compounds of the homologous series of Aurivillius phases, for example, in Bi_2NbO_5F.[104] Comparison of the interlayer distances in the Bi_2O_2 blocks in the Bi2201 phase and in the $Bi_2O_2F_2$ block of the Aurivillius phase accounts for the increase in the unit cell parameter *c* from 24.35 to 26.18 Å upon fluorination. The distance between two bismuth-containing layers located above and below the interlayer cavities is decreased from 3.18–3.20 Å in the starting Bi2201 phase to 2.49–2.56 Å in the fluorinated Bi2201 phase. This decrease is caused by Coulombic interactions between the anions in the interlayer cavities and the Bi^{3+} cations (Fig. 24). It should be noted that the oxygen atoms in the BiO layers experience repulsions from the interlayer anions. Hence, the BiO layers in the structure of the starting Bi2201 phase are nearly planar and the distance between the bismuth- and oxygen-containing sublayers of this layer along the *c* axis is no higher than 0.24–0.26 Å, whereas this distance in Aurivillius phases increases to 0.92–1.07 Å. This leads to splitting of the BiO layer into two layers one of which consists of the bismuth atoms and the other is composed of the oxygen atoms. In spite of shortening of the distance between the layers containing the bismuth cations, the total increase in the size of the $Bi_2O_2F_2$ block reaches 0.7–1.0 Å, which must lead to an increase in the parameter *c* by 1.4–2.0 Å. An increase in the coordination number of bismuth in a fluorinated phase also leads to elongation of the Bi–O bond and an increase in the size of the block in the *ab* plane. As a result, the commensurability between the $Bi_2O_2F_2$ blocks and the CuO_2 layers is achieved thus diminishing modulations. It should be noted that the structure of the fluorinated Bi2201 phase is a hybrid combining the Bi-containing $Bi_2O_{2-x}F_{2+x}$ blocks (like in Aurivillius phases) and the perovskite-like $A_{2n}Ca_{n-1}Cu_nO_{2n+2}$ blocks ($n = 1$). Such phases belong to a new homologous series $Bi_2A_2Ca_{n-1}Cu_n(O,F)_{2n+6}$. The third representative of this series, *viz.*, $Bi_2Sr_2Ca_2Cu_3O_8F_4$, was prepared by treating the Bi2223 phase with $NH_4F \cdot HF$ (see Ref. 33) although the superstructure $\sqrt{2}a_p \times \sqrt{2}a_p$ is retained. The distance between the bismuth- and strontium-containing layers is increased from 2.7 Å in the starting phase to 3.6 Å in the fluorinated phase, whereas the distance between two adjacent bismuth-containing layers is decreased from 3.2 to 2.5 Å in the fluorinated phase. In the plane of the layer, the Bi–Bi distances are also elongated from 3.53 Å in the starting phase to 3.76 Å in the fluorinated phase.

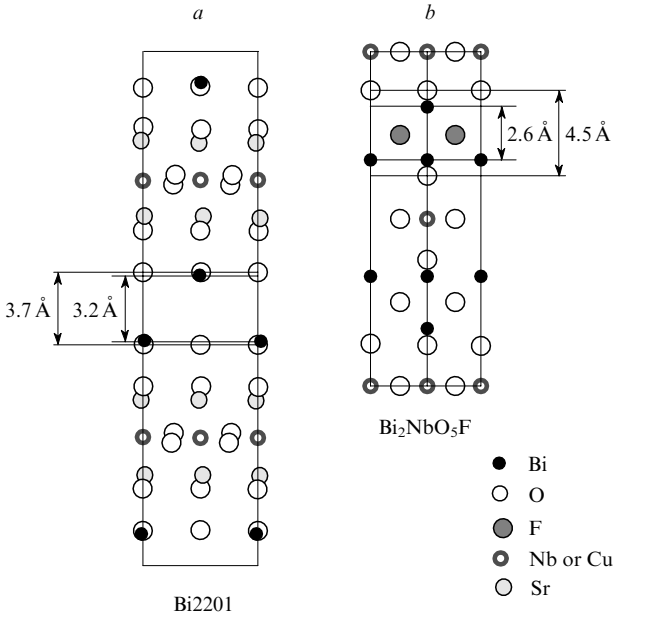


Figure 24. Crystal structures of the Bi2201 phase (*a*) and the Aurivillius phase Bi_2NbO_5F (*b*).

Fluorination of the Bi2201 and Bi2223 phases led to degradation of their superconducting properties. The $Bi_2Sr_{1.6}Ca_{0.4}.CuO_{6.33}$ compound ($T_c = 27$ K) lost superconductivity upon fluorination. In the Bi2223 phase (which is initially characterised by $T_c = 105$ K), the volume of the superconducting phase decreased and a second superconducting transition with $T_c = 75$ K was observed.

The advantage of the fluorinated Bi2201 phase over the starting compound in which the CuO_2 layers are substantially distorted is the absence of incommensurate modulations. Apparently, attainment of the optimum ratio between oxygen and fluorine with retention of these layers will allow one to prepare superconducting compounds based on oxyfluorides of a new homologous family.

V. Conclusion

Fluorination of complex cuprates can be used for the preparation of new compounds with structures necessary for superconducting properties to be manifested. In addition, fluorination of these compounds can be employed for attaining the required concentration of carriers (electrons or holes) in the conduction band. The character of the changes of the crystal structure upon fluorination is determined by the structural features of the starting compound and the amount of excessive anions. The following regularities can be noted:

– the replacement of oxygen atoms with an equivalent amount of fluorine atoms causes only slight changes to the unit-cell dimensions associated with a small difference in the ionic radii of O^{2-} and F^- and with elongation of the equatorial $Cu-O_{eq}$ bonds due to a decrease in the oxidation state of copper;

– the incorporation of excessive fluorine atoms and completion of the coordination polyhedron about the Cu^{2+} cations to an octahedron leads to substantial elongation of the axial $Cu-O$ bonds accompanied by an increase in the distances between the $Cu(O,F)_2$ and AO layers;

– the filling of anion vacancies in the structure with fluorine atoms diminishes structural distortions caused by ordering of the oxygen atoms and anion vacancies;

– location of fluorine atoms in the interlayer cavities induces rearrangement of the crystal structure to reduce Coulombic repulsions between the anions in the interlayer cavities and anions in the adjacent layers.

This review has been written with the financial support of the Russian State Scientific Program on Superconductivity 'Poisk', INTAS (Grant No. 99-1136), the Cooperative Research Development Foundation (Project No. 2256), and Volkswagen Stiftung (Grant No. I/75849). We thank V V Sokolov (Laboratory of Inorganic Synthesis, Institute of Applied Chemical Physics, Russian Research Centre 'Kurchatov Institute') and the research teams working at the Laboratory of Inorganic Crystal Chemistry of the Department of Chemistry of the M V Lomonosov Moscow State University and at the Laboratory of Electron Microscopy of the University of Antwerpen for helpful discussion and valuable advice. A M Abakumov and E V Antipov acknowledge the support of the Academic Council of the M V Lomonosov Moscow State University and the Charity Foundation for the Support of National Science of the Russian Academy of Sciences.

References

1. Antipov E V, in *Superconducting Materials: Advances in Technology and Applications* (Eds A Tampliery, G Celotti) (Singapore: World Scientific, 1998) p. 161
2. R D Shannon, C T Prewitt *Acta Crystallogr., Sect. B* **25** 925 (1969)
3. A C W P James, S M Zahurak, D W Murphy *Nature* (*London*) **338** 240 (1989)
4. J Sugiyama, Y Ojima, T Takata, K Sakuyama, H Yamauchi *Physica C* **173** 103 (1991)
5. J Sugiyama, M Kosuge, Y Ojima, H Yamauchi, S Tanaka *Physica C* **179** 131 (1991)
6. M Alexander, H Romberg, N Nuecker, P Adelmann, J Fink, J T Markert, M B Maple, S Uchida, H Takagi, Y Tokura, A C W P James, D W Murphy *Phys. Rev. B* **43** 333 (1991)
7. M E López-Morales, P M Grant *J. Solid State Chem.* **85** 159 (1990)
8. E E Fadeeva, E I Ardashnikova, M P Borzenkova, in *Proceedings of the International Workshop on Chemistry and Technology of High-Temperature Superconductors, Moscow, 1991* p. 52
9. C Wang, J Liang, X Chen, J Min, G Rao, C Dong, G Che, S Jia *Physica C* **260** 64 (1996)
10. M Isobe, J-Q Li, Y Matsui, F Izumi, Y Kanke, E Takayama-Muromachi *Physica C* **269** 5 (1996)
11. T Kawashima, Y Matsui, E Takayama-Muromachi *Physica C* **257** 313 (1996)
12. S R Ovshinsky, R T Young, D D Allred, G DeMaggio, G A Van der Leeden *Phys. Rev. Lett.* **58** 2579 (1987)
13. G V Bazuev, V N Krasil'nikov, V N Sukhanova *Zh. Neorg. Khim.* **38** 17 (1993) [a]
14. A K Tyagi, S J Patwe, U R K Rao R M Iyer *Solid State Commun.* **65** 1149 (1988)
15. T A Vanderah, D L Decker, D C Harris, B L Chamberland *Mater. Res. Bull.* **24** 121 (1989)
16. E E Fadeeva, E I Ardashnikova, B A Popovkin, M P Borzenkova *Zh. Neorg. Khim.* **38** 389 (1993) [a]
17. E I Ardashnikova, S V Lubarsky, D I Denisenko, R V Shpanchenko, E V Antipov, G Van Tendeloo *Physica C* **253** 259 (1995)
18. E I Ardashnikova, I M Vatsuro, R V Shpanchenko, E V Antipov *Zh. Neorg. Khim.* **43** 1712 (1998) [a]
19. M Al-Mamouri, P P Edwards, C Greaves, M Slaski *Nature (London)* **369** 382 (1994)
20. P R Slater, P P Edwards, C Greaves, I Gameson, M G Francescony, J P Hodges, M Al-Mamouri, M Slaski *Physica C* **241** 151 (1995)
21. M G Francesconi, P R Slater, J P Hodges, C Greaves, P P Edwards, M Al-Mamouri, M Slaski *J. Solid State Chem.* **135** 17 (1998)
22. A Tressaud, B Chevallier, B Lepine, K Amine, L Lozano, E Marquestaut, J Etourneau *Eur. J. Solid State Inorg. Chem.* **27** 309 (1990)
23. C Perrin, O Pena, M Sergent, G Fonteneau, J Lucas *Europhys. Lett.* **11** 181 (1990)
24. B M Tissue, K M Cirillo, J C Wright, M Daeumling, D C Larbalestier *Solid State Commun.* **65** 51 (1988)
25. P R Slater, J P Hodges, G M Francescony, C Greaves, M Slaski *J. Mater. Chem.* **7** 2077 (1997)
26. C Greaves, J L Kissik, M G Francescony, L D Aikens, L J Gillie *J. Mater. Chem.* **9** 111 (1999)
27. B Chevallier, A Tressaud, B Lepine, K Amine, J M Dance, L Lozano, E Hickey, J Etourneau *Physica C* **167** 97 (1990)
28. A Tighezza, J L Rehspringer, M Drillon *Physica C* **198** 209 (1992)
29. U Asaf, I Felner, U Yaron *Physica C* **211** 45 (1993)
30. S Adachi, X-J Wu, T Tamura, T Tatsuki, A Tokiwa-Yamamoto, K Tanabe *Physica C* **291** 59 (1997)
31. S Adachi, T Tatsuki, T Sugano, A Tokiwa-Yamamoto, K Tanabe *Physica C* **334** 87 (2000)
32. A K Tyagi, U R K Rao, R M Iyer, A K Rajarajan, L C Gupta *J. Mater. Sci. Lett.* **11** 1288 (1992)
33. E Bellingeri, G Grasso, R E Gladyshevskii, M Dhalle, R Flukiger *Physica C* **329** 267 (2000)
34. P Lightfoot, S Pei, J D Jorgensen, X-X Tang, A Manthiram, J B Goodenough *Physica C* **169** 15 (1990)
35. X Chen, J Liang, W Tang, C Wang, G Rao *Phys. Rev. B* **52** 16 233 (1995)
36. Y Jinling, L Jingkui, R Guanghui, Q Yueling, S Ying, T Weihua *Physica C* **270** 35 (1996)
37. P R Slater, J P Hodges, M G Francesconi, P P Edwards, C Greaves, I Gameson, M Slaski *Physica C* **253** 16 (1995)
38. J-H Choy, W Lee, S-J Hwang *Physica C* **322** 93 (1999)
39. R Suryanarayanan, R Nagarajan, H Selig, L Ben-Dor *Physica C* **361** 40 (2001)
40. M Takashima, S Yonezawa, M Aoyama, M Matsumiya *J. Fluorine Chem.* **97** 247 (1999)
41. *IVTANTHERMO, Database of Thermodynamic Properties of Individual Substances* (Moscow: THERMOCENTER, Russian Academy of Sciences, 1993)

42. Yu M Kiselev *Vestn. Mosk. Univ., Ser. 2, Khim.* **39** 3 (1998) [b]
43. Yu M Kiselev *Koord. Khim.* **23** 83 (1997) [c]
44. R V Shpanchenko, M G Rozova, A M Abakumov, E I Ardashnikova, M L Kovba, S N Putilin, E V Antipov, O I Lebedev, G Van Tendeloo *Physica C* **280** 272 (1997)
45. A Krol, Y L Soo, Z H Ming, S Huang, Y H Kao, G C Smith, K Lee, A C W P James, D W Murphy *Phys. Rev. B* **46** 443 (1992)
46. C H Chen, D J Werder, A C W P James, D W Murphy, S Zahurak, R M Fleming, B Batlogg, L F Schneemeyer *Physica C* **160** 375 (1989)
47. E Z Kurmaev, V R Galakhov, V V Fedorenko, L V Elokhina, S Bartkowski, M Neumann, C Greaves, P Edwards, M Al-Mamouri, D L Novikov *Phys. Rev. B* **52** 2390 (1995)
48. D R Lines, M T Weller, D B Currie, D M Ogborne *Mater. Res. Bull.* **26** 323 (1991)
49. J T Vaughey, J B Wiley, K R Poppelmeier *Z. Anorg. Allg. Chem.* **598**/**599** 321 (1991).
50. G Roth, P Adelmann, R Knitter, S Massing, Th Wolf *J. Solid State Chem.* **99** 376 (1992).
51. T G N Babu, C Greaves *J. Supercond.* **8** 21 (1995)
52. C Perrin, A Dinia, O Pena, M Sergent, P Burlet, J Rossat-Mignod *Solid State Commun.* **76** 401 (1990)
53. J L MacManus, D J Fray, J E Evetts *Physica C* **184** 172 (1991)
54. C Perrin, O Pena, M Sergent, P S Cristensen, G Fonteneau, J Lucas *Physica C* **934**–**935** 153 (1988)
55. K M Cirillo, J C Wright, J Seuntjens, M Dauemling, D C Larbalestier *Solid State Commun.* **66** 1237 (1988)
56. J R LaGraff, E C Behrman, J A T Taylor, F J Rotella, J D Jorgensen, L Q Wang, P G Mattoks *Phys. Rev. B* **39** 347 (1989)
57. T Kistenmacher *Phys. Rev. B* **36** 7197 (1987)
58. G Van Tendeloo, O I Lebedev, R V Shpanchenko, E V Antipov *J. Electron Microsc.* **1** 23 (1997)
59. A M Abakumov, M G Rozova, R V Shpanchenko, M L Kovba, S N Putilin, E V Antipov, O I Lebedev, G Van Tendeloo, E M Kopnin, J Karpinski *Physica C* **301** 155 (1998)
60. P N Oleinikov, R V Shpanchenko, M G Rozova, A M Abakumov, E V Antipov, I Khadermann, O I Lebedev, G Van Tendeloo *Zh. Neorg. Khim.* **46** 197 (2001) [a]
61. E V Antipov, A M Abakumov, V L Aksenov, A M Balagurov, S N Putilin, M G Rozova *Physica B* **241** 773 (1998)
62. Y T Wang, A M Hermann *Physica C* **254** 1 (1995)
63. X-G Wang, Z Huang, L Yuan *Physica C* **253** 254 (1995)
64. A M Abakumov, V L Aksenov, V A Alyoshin, E V Antipov, A M Balagurov, D A Mikhailova, S N Putilin, M G Rozova *Phys. Rev. Lett.* **80** 385 (1998)
65. A A Gippius, E N Morozova, E V Antipov, A M Abakumov, M G Rozova, K Luders, W Hoffmann, G Buntkowsky, O Klein *Phys. Rev. B* **61** 14 370 (2000)
66. E N Morozova, A A Gippius, E V Antipov, K Luders, W Hoffmann *Physica B* **284**–**288** 869 (2000)
67. A A Gippius, E V Antipov, O Klein, K Luders *Physica B* **284**–**288** 935 (2000)
68. V L Aksenov, A M Balagurov, V V Sikolenko, V G Simkin, V A Alyoshin, E V Antipov, A A Gippius, D A Mikhailova, S N Putilin, F Bouree *Phys. Rev. B* **55** 3966 (1997)
69. V L Aksenov, A M Balagurov, B N Savenko, D V Sheptyakov, V P Glazkov, V A Somenkov, S Sh Shilstein, E V Antipov, S N Putilin *Physica C* **275** 87 (1997)
70. Y Cao, Q Xiong, Y Y Xue, C W Chu *Phys. Rev. B* **52** 6854 (1995)
71. S N Putilin, E V Antipov, A M Abakumov, M G Rozova, K A Lokshin, D A Pavlov, A M Balagurov, D V Sheptyakov, M Marezio *Physica C* **338** 52 (2000)
72. K A Lokshin, D A Pavlov, S N Putilin, E V Antipov, D V Sheptyakov, A M Balagurov *Phys. Rev. B* **63** 064 511 (2001)
73. J L Wagner, B A Hunter, D G Hinks, J D Jorgensen *Phys. Rev. B* **51** 15 407 (1995)
74. G B Peacock, I Gameson, M Slaski, J J Capponi, P P Edwards *Physica C* **289** 153 (1997)
75. J-P Loquet, J Perret, J Fompeyrine, E Machler, J W Seo, G Van Tendeloo *Nature (London)* **394** 453 (1998)
76. A R Armstrong, W I F Daviv, I Gameson, P P Edwards, J J Capponi, P Bordet, M Marezio *Phys. Rev. B* **52** 15 551 (1995)
77. E V Antipov, J J Capponi, C Chaillout, O Chmaissem, S M Loureiro, M Marezio, S N Putilin, A Santoro, J L Tholence *Physica C* **218** 348 (1993)
78. A L Kharlanov, I Bryntse, E V Antipov, A V Luzikova *Acta Chem. Scand.* **47** 434 (1993)
79. A V Luzikova, A L Kharlanov, E V Antipov, H Müller-Bushbaum *Z. Anorg. Allg. Chem.* **620** 326 (1994)
80. A L Kharlanov, E V Antipov, I Bryntse, A V Luzikova, L M Kovba *Eur. J. Solid State Inorg. Chem.* **29** 1041 (1992)
81. J Hadermann, G Van Tendeloo, A M Abakumov, B Ph Pavljuk, M Rozova, E V Antipov *Int. J. Inorg. Mater.,* **2** 493 (2000)
82. K Otzschi, Y Ueda *J. Solid State Chem.* **107** 149 (1993)
83. L Er Rakho, C Michel, B Raveau *J. Solid State Chem.* **73** 514 (1988)
84. A M Abakumov, J Hadermann, M G Rozova, B Ph Pavljuk, E V Antipov, O I Lebedev, G Van Tendeloo *J. Solid State Chem.* **149** 189 (2000)
85. M H Tuilier, B Chevalier, A Tressaud, C Brisson, J L Soubeyroux, J Etourneau *Physica C* **200** 113 (1992)
86. A Tressaud, B Chevalier, L Piraux, M Cassart *J. Fluorine Chem.* **72** 165 (1995)
87. A M Abakumov, J Hadermann, G Van Tendeloo, R V Shpanchenko, P N Oleinikov, E V Antipov *J. Solid State Chem.* **142** 440 (1999)
88. C Chaillout, S W Cheong, Z Fisk, M S Lehmann, M Marezio, B Morozin, J E Schirber *Physica C* **158** 183 (1989)
89. F Izumi, Y-I Kim, E Takayama-Muromachi, T Kaniyama *Physica C* **235**–**240** 841 (1994)
90. V Bhat, J M Honig *Mater. Res. Bull.* **30** 1253 (1995)
91. M Cassart, E Grivei, J-P Issi, E Ben Salem, B Chevalier, C Brisson, A Tressaud *Physica C* **213** 327 (1993)
92. F Well, B Chevallier, M Chambon, A Tressaud, B Darriet, J Etourneau, G Van Tendeloo *Eur. J. Solid State Inorg. Chem.* **30** 1095 (1993)
93. S Adachi, T Tatsuki, T Tamura, K Tanabe *Chem. Mater.* **10** 2860 (1998)
94. J Hadermann, G Van Tendeloo, A M Abakumov, M G Rozova, E V Antipov *J. Solid State Chem.* **157** 56 (2001)
95. A M Abakumov, E V Antipov, L M Kovba, E M Kopnin, S N Putilin, R V Shpanchenko *Usp. Khim.* **64** 769 (1995) [*Russ. Chem. Rev.* **64** 719 (1995)]
96. L Rukang, C Greaves *Physica C* **339** 148 (2000)
97. J Hadermann, A M Abakumov, O I Lebedev, G Van Tendeloo, M G Rozova, R V Shpanchenko, B Ph Pavljuk, E M Kopnin, E V Antipov *J. Solid State Chem.* **147** 647 (1999)
98. X-D Xiang, S McKernan, W A Vareka, A Zettl, J L Corkill, T W Barbee III, M L Cohen, *Nature (London)* **348** 145 (1990)
99. N Kijima, R Gronsky, X-D Xiang, W A Vareka, J Hou, A Zettl, J L Corkill, M L Cohen *Physica C* **198** 309 (1992)
100. S-J Hwang, N-G Park, D-H Kim, J-H Choy *J. Solid State Chem.* **138** 66 (1998)
101. X -D Xiang, A Zettl, W A Vareka, J L Corkill, T W Barbee III, M L Cohen *Phys. Rev. B.* **43** 11 496 (1991)
102. T Kijima, H Sushida, M Yada, M Machida *J. Solid State Chem.* **141** 452 (1998)
103. J Hadermann, N R Khasanova, G Van Tendeloo, A M Abakumov, M G Rozova, A M Alekseeva, E V Antipov *J. Solid State Chem.,* **156** 445 (2001)
104. B Aurivillius *Ark. Kemi* **5** 519 (1952)

[a] — *Russ. J. Inorg. Chem. (Engl. Transl.)*
[b] — *Moscow Univ. Bull. (Engl. Transl.)*
[c] — *Russ. J. Coord. Chem. (Engl. Transl.)*